NASA TECHNICAL MEMORANDUM

NASA TM X-3523

NASA TM X-3523

6670-NEWTON ATTITUDE-CONTROL THRUSTER USING HYDROGEN-OXYGEN PROPELLANT

Larry H. Gordon

Lewis Research Center
Cleveland, Ohio 44135

NATIONAL AERONAUTICS AND SPACE ADMINISTRATION • WASHINGTON, D. C. • MAY 1977

1. Report No.	2. Government Accession No.	3. Recipient's Catalog No.
NASA TM X-3523		

4. Title and Subtitle	5. Report Date
6670-NEWTON ATTITUDE-CONTROL THRUSTER USING HYDROGEN-OXYGEN PROPELLANT	May 1977
	6. Performing Organization Code

7. Author(s)	8. Performing Organization Report No.
Larry H. Gordon	E-8981
	10. Work Unit No.
	506-21

9. Performing Organization Name and Address	11. Contract or Grant No.
Lewis Research Center National Aeronautics and Space Administration Cleveland, Ohio 44135	
	13. Type of Report and Period Covered
12. Sponsoring Agency Name and Address	Technical Memorandum
National Aeronautics and Space Administration Washington, D. C. 20546	14. Sponsoring Agency Code

15. Supplementary Notes

16. Abstract

As part of a program to develop a reusable, attitude-control propulsion system for the space transportation system, a flight weight, gaseous-hydrogen - gaseous-oxygen attitude-control thruster assembly was tested. This report describes the NASA testing of one of four contractor-built thrusters to obtain data on cyclic life, thermal and hydraulic characteristics, pulse response, and performance. The basic thruster components were tested in excess of 51 000 pulses and 660 seconds, steady state, with no degradation of the 93 percent characteristic exhaust velocity efficiency level. Nominal operating conditions were a chamber pressure of 207 N/cm^2 (300 psia), a mixture ratio of 4.0, a pulse width of 100 ms, and a pulse frequency of 2 Hz.

17. Key Words (Suggested by Author(s))	18. Distribution Statement
Rocket engines	Unclassified - unlimited STAR Category 20

19. Security Classif. (of this report)	20. Security Classif. (of this page)	21. No. of Pages	22. Price*
Unclassified	Unclassified	37	A03

* For sale by the National Technical Information Service, Springfield, Virginia 22161

6670-NEWTON ATTITUDE-CONTROL THRUSTER USING HYDROGEN-OXYGEN PROPELLANT

by Larry H. Gordon

Lewis Research Center

SUMMARY

The flight-weight, gaseous-hydrogen - gaseous-oxygen attitude-control propulsion system (ACPS) thruster employs a spark-initiated igniter and poppet main-propellant valves. The nominal engine operating conditions are: 6672 N (1500 lb) thrust, 207-newton-per-square-centimeter (300-psia) chamber pressure, 4.0 mixture ratio, 276-newton-per-square-centimeter (400-psia) valve-inlet pressure, 139 K (250^{o} R) hydrogen-inlet temperature, and 208 K (375^{o} R) oxygen-inlet temperature. This report pertains to the NASA testing of one of four ACPS engines fabricated by the Aerojet Liquid Rocket Company for NASA.

The objective of the testing was to obtain data, in addition to that of the contractor, on the performance, thermal and hydraulic characteristics, pulse response, and cyclic life. The basic thruster components, injector and chamber, were tested in excess of 51 000 pulses and 660 seconds, steady state, for an overall firing accumulation of over 6678 seconds with no degradation of the 93 percent characteristic exhaust-velocity efficiency. The pulse duration was 100 milliseconds with a frequency of 2 hertz. The thruster assembly, as tested, consisted of a premix triplet injector (F-O-F), a regeneratively cooled chamber using 79 percent of the hydrogen flow and a film-cooled throat and skirt, an oxygen-rich torch igniter, an integral exciter (capacitive discharge) spark plug; two igniter valves, and two main-propellant valves. The injector was made of stainless-steel body with nickel face plate. The chamber had a zirconium-copper liner and an Armco 22-13-5 stainless-steel shell. The igniter body was nickel, and the throat and nozzle were spun from Haynes 188 alloy.

As a result of the test program, it was recommended that some minor inspection, fabrication, and design modifications be incorporated in future ACPS engines. These results, coupled with the demonstrated performance and life, have provided a data base for reliable, reusable, attitude-control thrusters as contemplated for future, cryogenic space-transportation vehicles.

INTRODUCTION

As part of the NASA's goal of reusable space transportation systems, a program was conducted through contracts to advance the technology of hydrogen-oxygen thrusters applicable to the Space Shuttle attitude control propulsion system (ACPS). This effort was sponsored by the Office of Aeronautics and Space Technology and managed by the Lewis Research Center. At the beginning of the thruster technology program, hydrogen-oxygen propellants were chosen for the Space Shuttle ACPS for both the orbiter and booster stages. Subsequently, the Shuttle concept changed from the reusable flyback booster and internally tanked orbiter to the present external tank orbiter with twin solid-rocket-motor boosters. Because of these configuration changes, which reduced the ACPS total system impulse requirements, earth storables were selected as baseline ACPS propellants. The hydrogen-oxygen technology was continued, but on a reduced scale, to insure a strong technology base for a proposed modification II, all-cryogenic, Shuttle and other possible future launch vehicle applications. Estimates of nominal operation conditions and performance goals for which the thrusters were designed are shown in tables I and II.

Initially, NASA contracted with Bell Aerospace (ref. 1), Rocketdyne (refs. 2 to 4), TRW Systems (refs. 5 to 8), Marquardt (ref. 9), and Aerojet (refs. 10 and 11) to investigate various injection techniques, cooling concepts, and ignition modes for the ACPS thrusters. (See ref. 12 for a review of these studies.) The Aerojet ACPS configuration

TABLE I. - ENGINE OPERATING CONDITIONS

[Nominal design values.]

Thrust, N (lbf)	6672 (1500)
Chamber pressure, N/cm^2 (psia)	207 (300)
Mixture ratio	4.0
Nozzle expansion ratio	40.1
Propellant inlet temperature, K (^{o}R):	
Hydrogen	139 (250)
Oxygen	208 (375)
Propellant inlet pressure (to valve), N/cm^2 (psia):	
Hydrogen	274 (400)
Oxygen	276 (400)
Specific impulse, N · s/kg (lbf · s/lbm):	
Steady state	4266 (435)
Pulsing average	3923 (400)

TABLE II. - ENGINE DESIGN REQUIREMENTS

Fuel	Gaseous hydrogen derived from vaporization of liquid hydrogen
Oxidizer	Gaseous oxygen derived from vaporization of liquid oxygen
Installation	Buried within vehicle mold line
Maximum external temperature	260° C (500° F)
Total life capability	Estimated 2500 min
Total number of firings	Estimated 500 000 pulses plus 25 000 deep thermal cycles (full temperature range on each component)
Maximum single firing duration	500 s
Compatibility	Compatible with propellants, test fluids, cleaning fluids, and environmental contaminants for 10-year life requirement
Reusability	To be reusable with minimum servicing and refurbishment
Service and maintenance	Design for ease of service and maintenance when required
Minimum impulse bit (goal)	222 N · s (50 lbf-s)
Response	50 ms (time from electrical signal to 90 percent thrust)
Reentry heating (goals)	30 min of exposure per mission to following temperatures: At nozzle exit plane, 982° C (1800° F) At chamber throat, 649° C (1200° F)
Nozzle scarfing capability	Nozzle skirt shall be easily scarfed beyond an expansion ratio of 25:1
Weight goal for complete thruster assembly less valves	6804 g (15 lbm)

was selected for the investigation of chamber and injector life, pulse-mode operation with cold propellants, the effects of valve sequencing, and the optimization of minimum weight and cycle life relative to performance. Four 6672-newton (1500-lb) thrust engines (fig. 1) - two for testing at Aerojet, one for testing at Lewis, and one as a backup - were built by Aerojet. The Aerojet tests accumulated over 42 000 pulses (ref. 13). The objectives of the testing of the ACPS thruster at Lewis was to obtain additional data on performance, thermal and hydraulics characteristics, pulse response, and cyclic life and to demonstrate the Shuttle ACPS mission requirements of a minimum of 500 firings per mission for 100 flights for a total of 50 000 pulse firings. This report documents the Lewis test program.

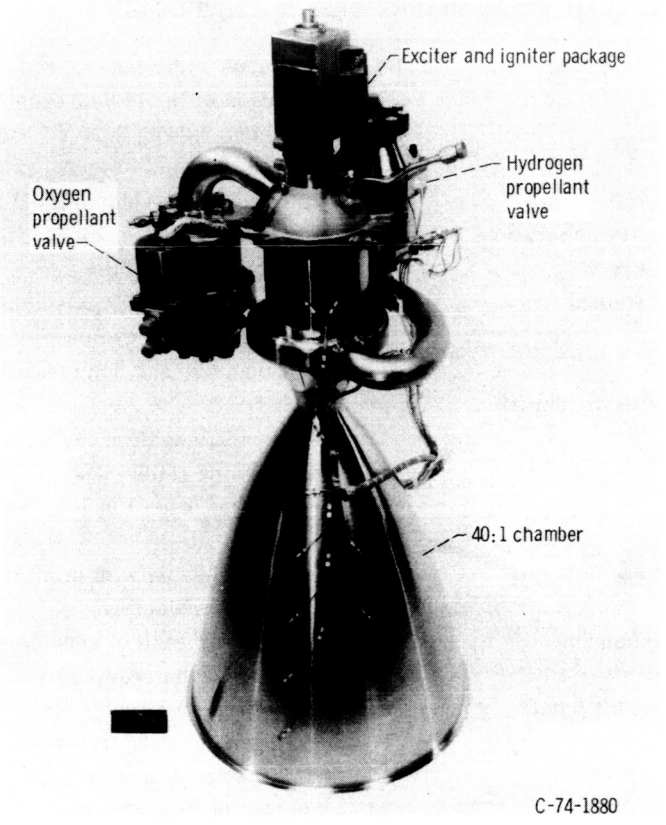

Figure 1. - ACPS thruster assembly.

DESCRIPTION OF TEST HARDWARE

A description of the ACPS thruster including fabrication procedures is contained in reference 13. The following sections briefly describe each ACPS component so that later references to instrumentation locations, problem areas, and hardware modifications will be clear. The major components to be discussed are the igniter, injector, chamber, and valves.

Igniter

The igniter (fig. 2) consists of a spark plug, which is integral with the capacitive discharge exciter, and a combustion chamber (tube) made of nickel 201. The igniter uses an air-gap spark plug which discharges into an oxidizer-rich environment having a mixture ratio O/F of 41. Additional hydrogen (fuel) is added downstream of this igni-

tion source to obtain an O/F of 5.4 at the injector face plane. The spark igniter operated at an energy level of 100 millijoules at a fixed gap breakdown voltage of 20 000 volts. The gap size was 0.0762 centimeter (0.030 in.). Input voltage was 28±4 volts, direct current, and the spark rate was 500 sparks per second. (See the Results section for modifications to design as a result of life testing.)

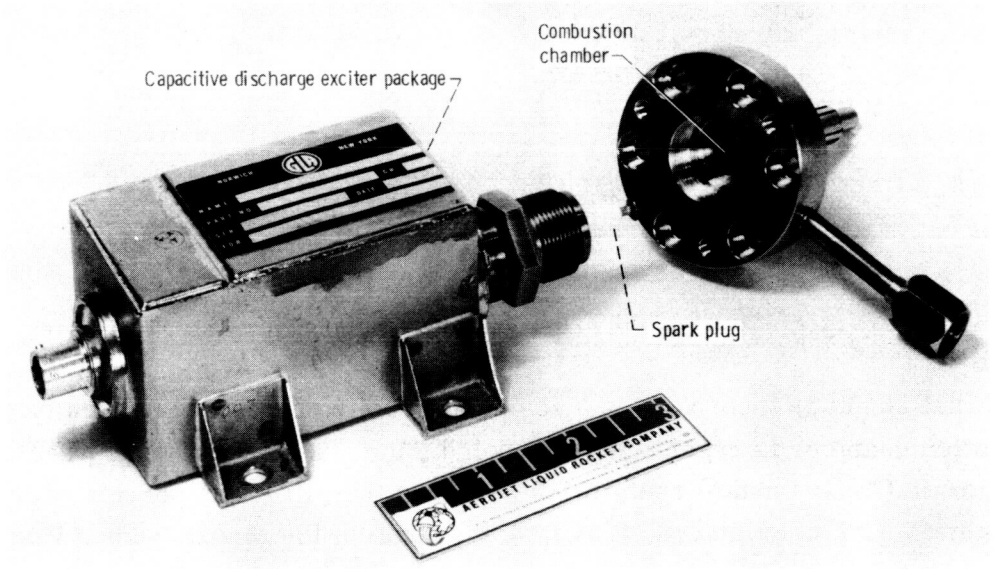

Figure 2. - Spark igniter (air-gap and capacitive discharge).

Injector

The injector shown in figure 3 is a premix design (fuel and oxidizer mixed slightly upstream of the injector face plane) that uses etched platelets to form the fuel orifices and face coolant channels. The fuel circuit is fed directly from the thrust chamber coolant passage outlets. The oxidizer is supplied from a domeshaped manifold, which contains distribution plates to insure uniform oxidizer distribution. Seventy-two oxidizer tubes extend from the oxidizer dome through the fuel plenum to the face. The spark-augmented torch igniter discharges in the center of the injector face. The entire injector body is made from AISI 304 L stainless steel, and the etched face plates are made from nickel 200. The injector is joined to the thrust chamber by an external weld with a piston ring seal between the injector face and the chamber wall.

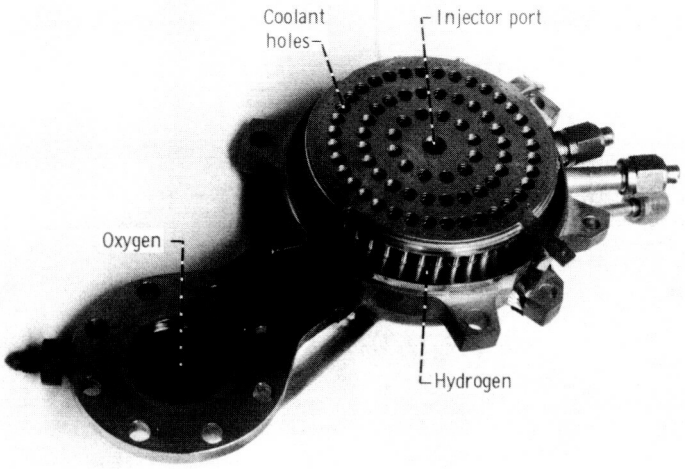

Figure 3. - ACPS injector (72 premixing elements).

Thrust Chamber

The thrust chamber incorporates a composite cooling system. The major portion of the combustion chamber is regeneratively cooled (80 channels) with fuel. The convergent liner and nozzle (figs. 4 and 5) contain 160 passages that direct 21 percent of the fuel flow to a station 3.81 centimeters (1.50 in.) upstream of the throat, where it is introduced as a film coolant. The throat and entire divergent nozzle are of spun Haynes 188 material. The gas-side wall material in the cooled areas ahead of the fuel-film-coolant injection station is a zirconium-copper alloy that contains rectangular coolant passages. These are closed out by an Armco 22-13-5 stainless-steel shell, which is brazed to the copper liner. The stainless-steel shell is joined to the injector and adiabatic wall nozzle by welding. The composite cooling system results in the fuel-inlet manifold (which is also made from Armco 22-13-5 stainless steel) being located at the entrance to the convergent nozzle. The thrust chamber parts are shown in figure 6 before the welding operations that form the complete thrust chamber assembly.

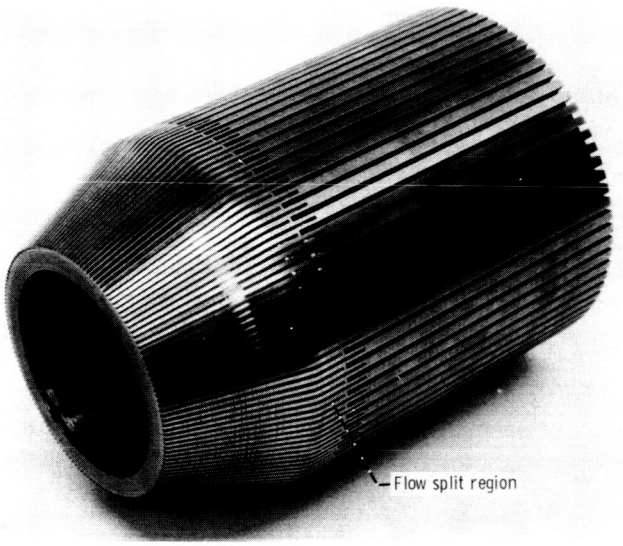

Figure 4. - Convergent chamber liner (Amzirc alloy).

Figure 5. - Convergent nozzle shell without liner (Armco 22-13-5).

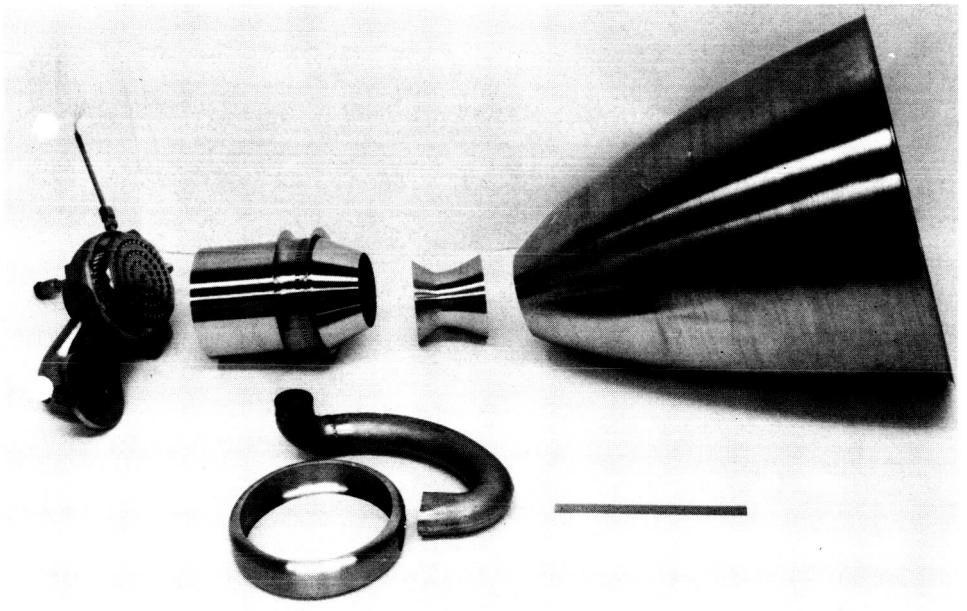

Figure 6. - Injector and chamber assembly (before welding).

Main Propellant Valves

The main propellant valves were designed by the Marquardt Co. under contract to Lewis (ref. 9). A photograph of the valve assembly and a design schematic are shown in figures 7 and 8. This valve is of the coaxial poppet configuration and features an integral, three-way pilot valve. Examination of figure 8 shows that the effective bellows diameter is greater than the effective sealing diameter is acted upon by the valve inlet pressure to cause an opening force upon the poppet and bellows assembly. This force accelerates the poppet until it strikes the impact absorber. Once the pressure downstream of the valve builds up, an increased pressure force is available to lock the the poppet in the open position. To close the valve, the left side of the poppet is simply repressurized with the valve inlet pressure by means of the three-way pilot valve. This force, in combination with the spring forces from the axial guidance flexure and the bellows, returns the poppet to the closed position. A poppet stop minimizes the impact energy imposed on the valve seat. The valve seat, in effect, is mounted on a spring support structure that controls the poppet and seat interface load when the poppet valve is in the closed position. Guidance of the poppet and bellows assembly during the opening and closing motions is provided by means of an axial guidance flexure assembly which, in turn, is supported on a centrally located shaft rigidly attached to the outlet of the valve. A mechanical tang incorporated in the nut makes this shaft assembly rigid to prevent the nut from loosening during valve cycling.

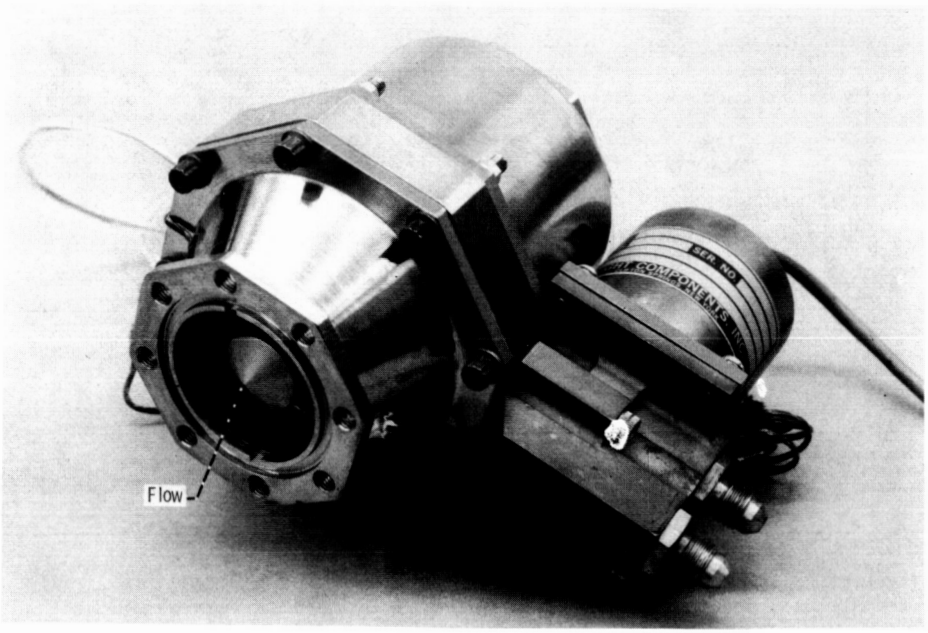

Figure 7. - Main propellant valve.

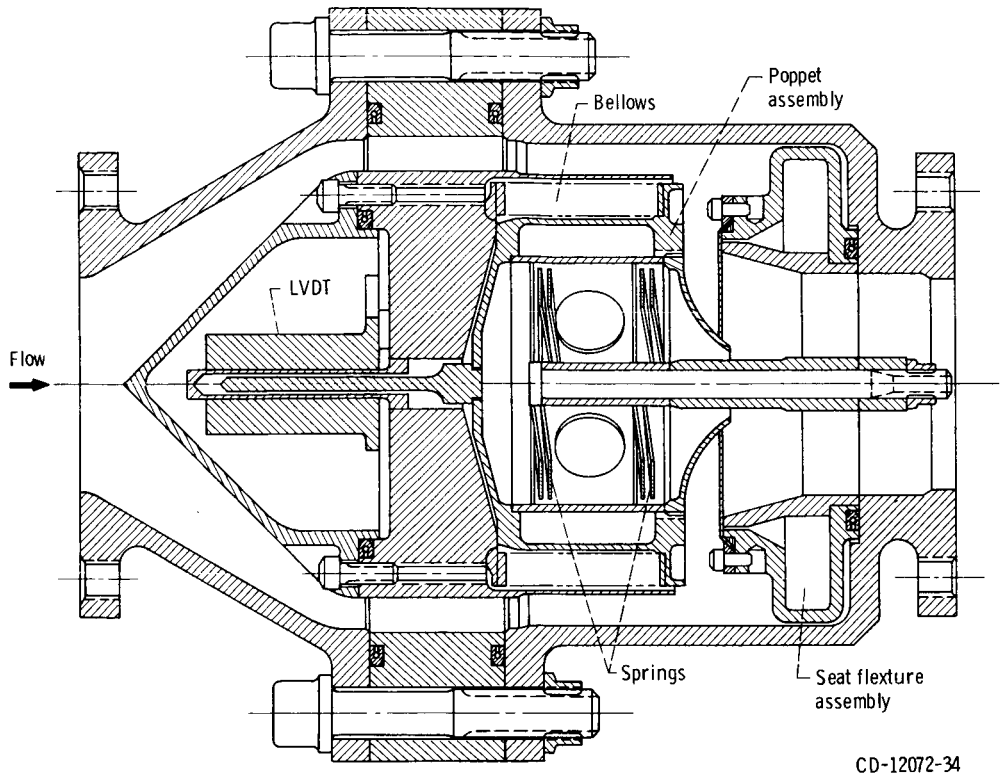

Figure 8. - Main propellent valve. (Vent to open; pressurize to close.)

The valve configuration (fig. 7) also features an integral, electromechanical transducer (LVDT) to monitor valve position. Although the valve mechanism of the three-way pilot valve is an integral part of the main valve, the solenoid actuator required to operate the pilot valve is still located outside of the main valve and can be easily removed.

The principal material of construction is Inco 718, heat-treated and welded in the heat-treated conditions. Other materials used in the construction of this valve are AISI 321 stainless steel for the pilot valve inlet tubing, polyimide for the valve seats, AISI 430 stainless steel for magnetic parts of the solenoid, AISI 303/304 stainless steel for the nonmagnetic parts of the solenoid, a 440C stainless steel ball for the pilot valve poppet, copper and Nichrome for the coil wiring in the solenoid, Carpenter HP 49 for the LVDT armature, AISI 316 stainless steel for the LVDT pressure vessel, AISI 304 stainless steel for LVDT cover, and copper for the windings in the LVDT.

DESCRIPTION OF TEST FACILITY

The tests were conducted in the Lewis rocket laboratory test facility, which was modified to provide the conditioned propellants and engine controls necessary for the successful operation of the ACPS thruster.

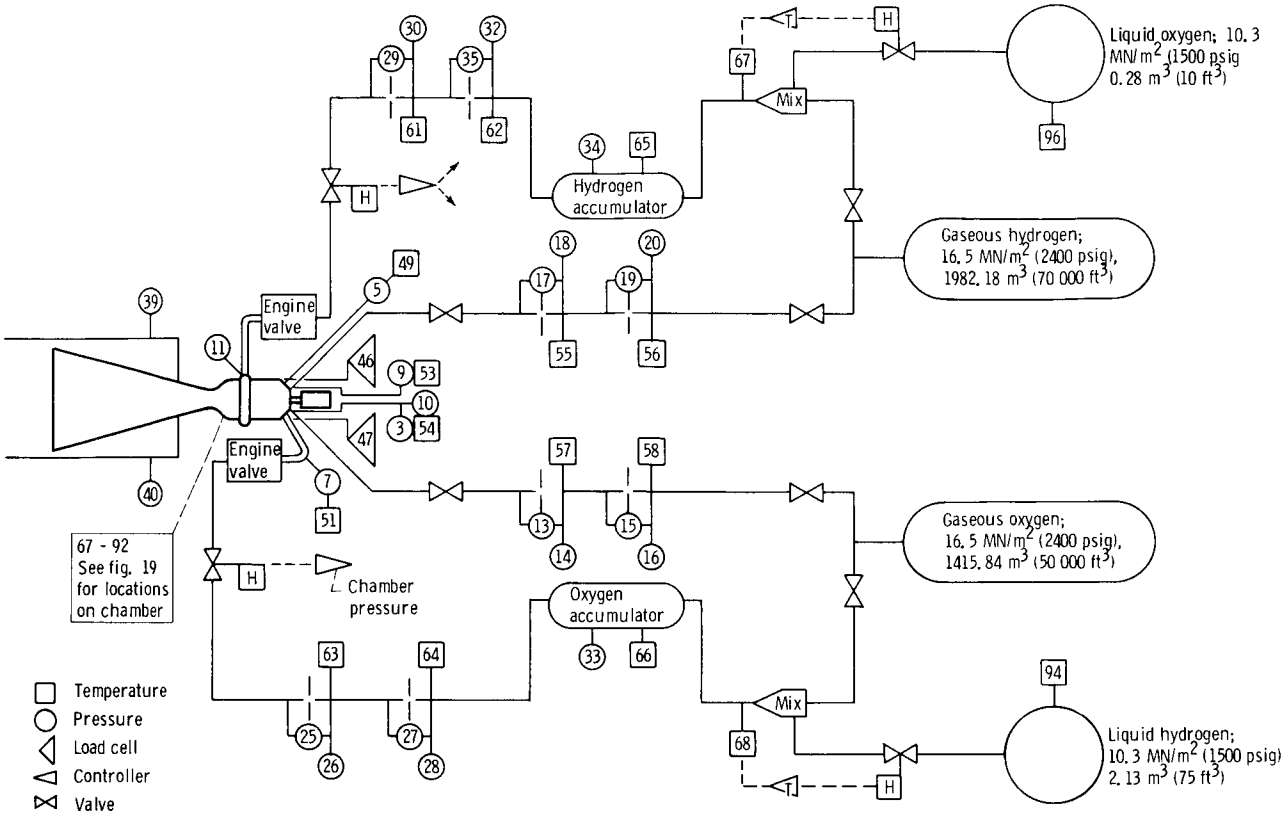

Figure 9. - ACPS test installation schematic. (See table III.)

The conditioned propellants were obtained by blending the respective propellants in their liquid and gaseous states as shown in the test installation schematic (fig. 9). In addition to this temperature control, the system incorporated chamber pressure and mixture ratio controllers. The nominal 13 344-newton (3000-lbf) thrust stand was operated in a sea level or altitude mode by the attachment of a graphite exhaust diffuser (figs. 10 and 11).

One hundred data acquisition channels were available for recording the pressures and temperatures. (See table III.) With five-point averaging of the data, the data reduction system recorded a set of data every 100 milliseconds for steady-state testing. In the pulse mode testing the number of data channels (table III) was reduced to 50, which provided a nonaveraged data time slice every 10 milliseconds. Critical parameters, such as chamber pressure, were supercommutated to provide data points in 5 millisecond increments.

To insure accurate and precise time settings, a 12-channel digital timer (fig. 12) was used for both test modes. Ignition, valve times, etc., were set to within 1 millisecond. The number of pulses, pulse length (on-off), and number of pulses at cutoff

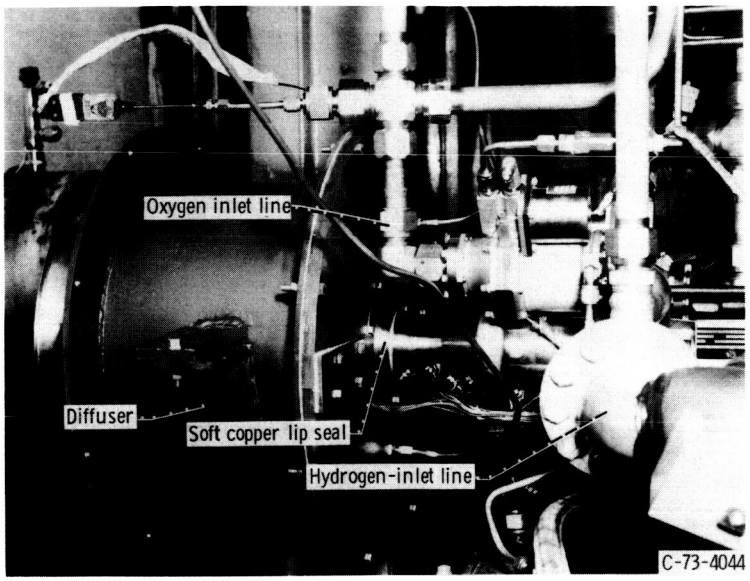

Figure 10. - C-21 test installation (nozzle diffuser attachment).

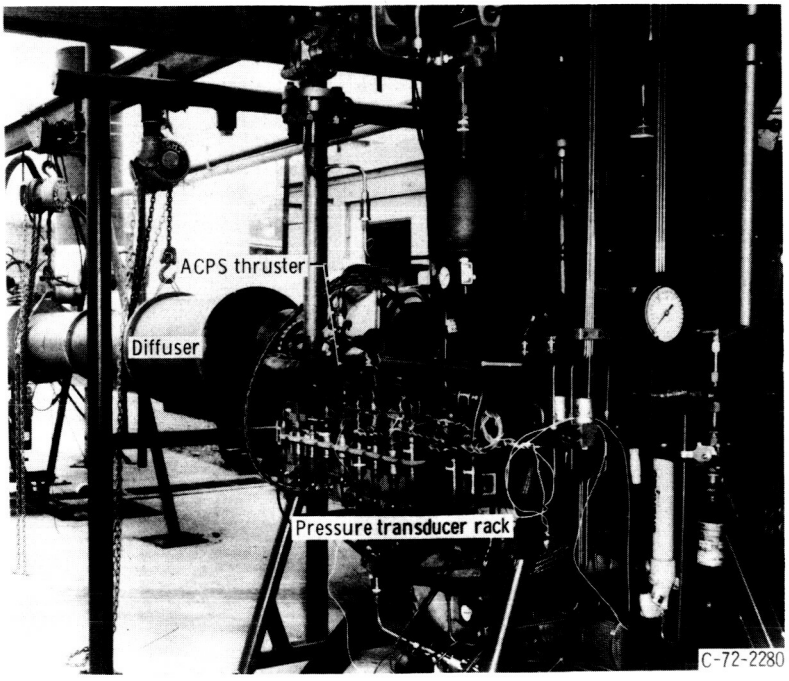

Figure 11. - C-21 test installation (diffuser and entire thruster assembly).

TABLE III. - INSTRUMENTATION LIST

Channel	Measurement	Type of instrument	Channel	Measurement	Type of instrument
[a]3	Chamber pressure	Strain gage bridge	57	Igniter oxidizer orifice temperature 1	Copper-constantan
[a]5	Fuel inlet pressure	↓	[a]58	Igniter oxidizer orifice temperature 2	↓
[a]7	Oxidizer inlet pressure	↓	61	Main fuel orifice temperature 1	↓
[a]9	Igniter fuel inlet pressure	↓	[a]62	Main fuel orifice temperature 2	↓
[a]10	Igniter oxidizer inlet pressure	↓	63	Main oxidizer orifice temperature 1	↓
[a]11	Regenerative coolant inlet pressure	↓	[a]64	Main oxidizer orifice temperature 2	↓
13	Igniter oxidizer delta pressure 1	↓	[a]65	Fuel accumulator temperature	↓
14	Igniter oxidizer static pressure 1	↓	[a]66	Oxidizer accumulator temperature	↓
[a]15	Igniter oxidizer delta pressure 2	↓	67	Fuel mix temperature	Chromel-constantan
[a]16	Igniter oxidizer static pressure 2	↓	68	Oxidizer mix temperature	Chromel-constantan
17	Igniter fuel delta pressure 1	↓	[a]69	Chamber temperature 11A	Chromel-Alumel
18	Igniter fuel static pressure 1	↓	[a]70	Chamber temperature 12A	↓
[a]19	Igniter fuel delta pressure 2	↓	[a]73	Injector manifold temperature 1	↓
[a]20	Igniter fuel static pressure 2	↓	[a]74	Injector manifold temperature 2	↓
25	Main oxidizer delta pressure 1	↓	[a]75	Injector face temperature 1	↓
26	Main oxidizer static pressure 1	↓	[a]76	Injector face temperature 2	↓
[a]27	Main oxidizer delta pressure 2	↓	[a]77	Chamber temperature 1A	↓
[a]28	Main oxidizer static pressure 2	↓	[a]78	Chamber temperature 1B	↓
29	Main fuel delta pressure 1	↓	[a]79	Chamber temperature 2A	↓
30	Main fuel static pressure 1	↓	[a]80	Chamber temperature 3A	↓
[a]32	Main fuel static pressure 2	↓	81	Chamber temperature 3B	↓
33	Oxidizer accumulator pressure	↓	[a]82	Chamber temperature 4A	↓
34	Fuel accumulator pressure	↓	83	Chamber temperature 4B	↓
[a]35	Main fuel delta pressure 2	↓	[a]84	Chamber temperature 5A	↓
[a]37	Exhaust diffuser pressure 1	↓	[a]85	Chamber temperature 6A	↓
40	Exhaust diffuser pressure 2	↓	[a]86	Chamber temperature 7A	↓
[a]45	Thrust 1	↓	87	Chamber temperature 7B	↓
46	Thrust 2	↓	[a]88	Chamber temperature 8A	↓
[a]49	Fuel inlet temperature	Copper-constantan	[a]89	Chamber temperature 9A	↓
[a]51	Oxidizer inlet temperature	↓	90	Chamber temperature 9B	↓
53	Igniter fuel inlet temperature	↓	[a]91	Chamber temperature 10A	↓
54	Igniter oxidizer inlet temperature	↓	92	Chamber temperature 10B	↓
55	Igniter fuel orifice temperature 1	↓	94	Liquid oxidizer temperature	Copper-constantan
[a]56	Igniter fuel orifice temperature 2	↓	96	Liquid fuel temperature	Rosin

[a]Parameters for pulse-mode testing.

or abort were set and monitored. Abort controls, usually ±10 percent of nominal value, were maintained on chamber pressure, fuel/oxidizer flows, and igniter oxidizer pressure.

The detection of subcritical crack growth was made through the use of the acoustic emission equipment (fig. 13). This dual channel system consisted of the following Dunegan/Endevco equipment:

(a) Two differential transducer sensors with preamplifiers (fixed 40-db gain)

(b) Two totalizers for basic data sampling with respective signal filtering and amplification equipment

(c) Both an audiomonitor and visual counter for emission output

(d) An analog x-y plotter for recording emission rate produced by a ramp generator and reset clock.

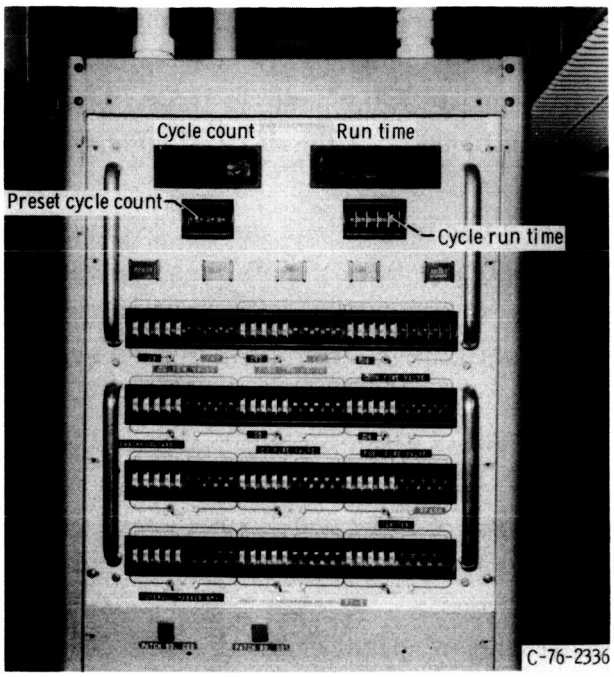

Figure 12. - Twelve-channel electronic timer (Δt = 0.001 s).

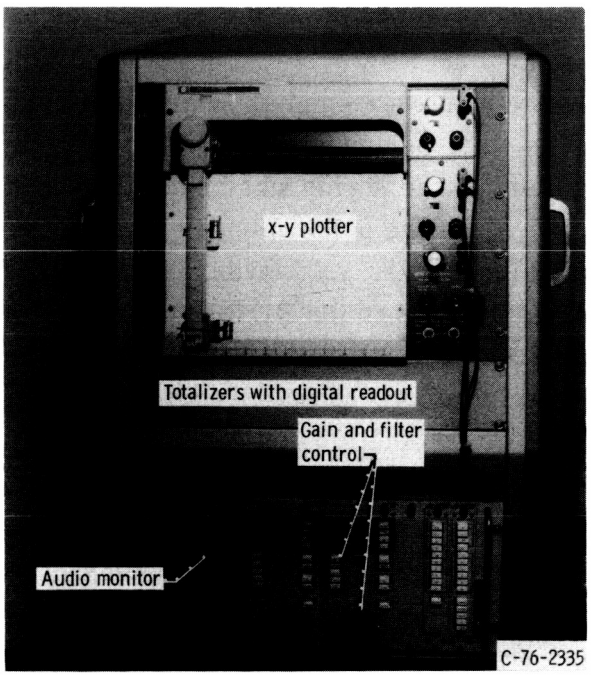

Figure 13. - Acoustic emission monitor (dual channel and plotter).

TEST PROCEDURES

Before testing the ACPS thruster, facility checkout tests were made using residual hardware from the previous technology programs (refs. 1, 2, 10, and 11). As a result of these check outs, a testing procedure was established for the ACPS thruster: At the start of each test slot an igniter-only test (timing trace, fig. 14(a)) was made. This was an important test because, as part of the nondestructive evaluation of the injector and chamber for cracks, the igniter had to be removed and the many assemblies and disassemblies of the ACPS increased the chance of human error and possible nonignition. To minimize the heat input to the chamber from the igniter exhaust, the firing was approximately 0.100 second with a 0.08-second fuel lag.

A 1.5-second steady-state test (fig. 14(b)) was then performed to insure that the desired chamber pressure, mixture ratio, and other operating parameters were obtained. As shown in figure 15 the data slice, common to all steady-state tests, was at constant operating conditions. This steady-state test was used, not only as a performance standard throughout the program, but also as a means of establishing set-point operations for the pulse-mode testing.

Because of the nominal 0.1-second on - 0.4-second off pulse-mode operation, it was not possible to retain the closed-loop control functions for chamber pressure P_c and mixture ratio O/F. Consequently, the set points, as established by the steady-state

tests, were used for P_c and O/F levels. Nevertheless, high and low P_c and flow control aborts were still maintained to insure the safety of the hardware. A typical pulse mode series is shown in figure 16 and the associated timing setup in figure 14(b). The pulse series was automatically controlled and continued until the desired number of pulses in the series was reached or manually terminated.

All of the pulse-mode and steady-state tests were performed with igniter oxidizer and fuel valves. However, in the real igniter it is desirable to eliminate these valves. As discussed in the RESULTS section, these valves were later eliminated, and valveless igniter tests were performed. The necessary changes to the existing timing sequence were minimal, as shown in figure 14(c).

On completion of a test slot (which usually consisted of a few steady-state tests and 1000 to 5000 pulses), the ACPS thruster was removed from the test facility and inspected. The inspection techniques used were (1) visual, (2) dye penetrant, and (3) acoustic emission. The dye penetrant (Dye Glo) was only used if a crack was indicated by either the visual or acoustic emission inspections.

The use of acoustic emission to detect crack growth in rocket chambers was new; consequently, the evaluation procedure was established by trial and error and was very qualitative.

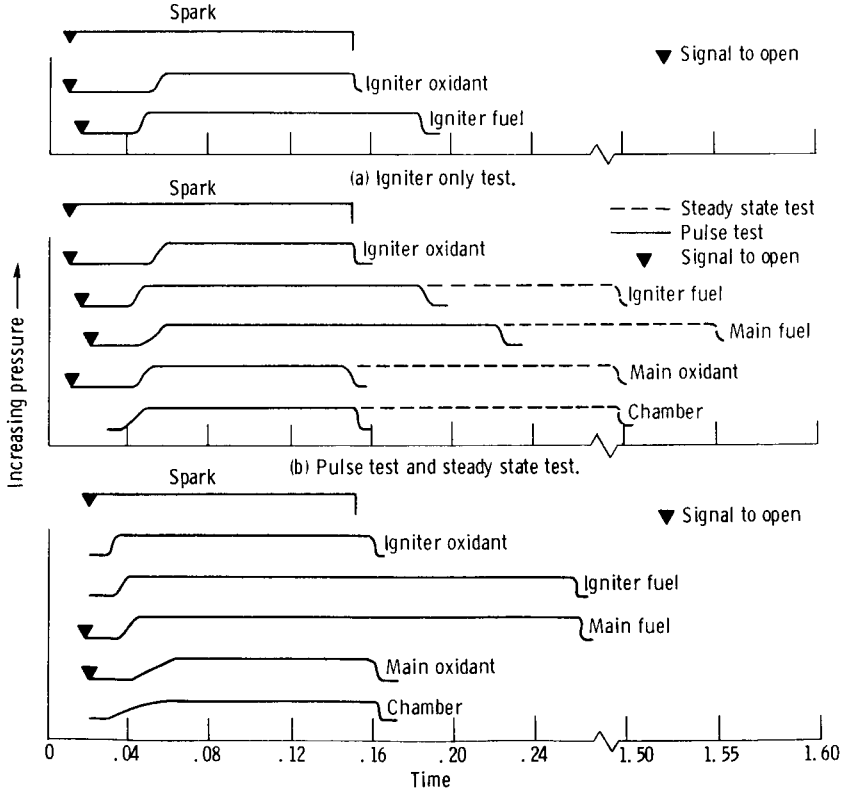

Figure 14. - Typical timing sequence and associated response time.

To cause any subcritical crack in the chamber to grow (i. e., emit noise), it was necessary to internally pressurize the thruster. This was accomplished by installing a throat plug and hydrostatically pressurizing the entire chamber and injector passages. A cleaning solvent, trichloroethane, was used as the pressurant to insure cleanliness.

Two transducers were attached to the ACPS chamber, one on the outside of the cylindrical portion of the combustion region (i. e., the chamber) and one on the coolant manifold. Initial tests were performed with both transducers attached to the chamber region. One was used to record total counts and one to record count rate. Because no significant data resulted from the count rate, this transducer was moved to the manifold to provide greater capability for detecting possible weld cracking. The transducers were attached by tape, and the adhesive was halocarbon grease, a completely halogenated chlorofluorocarbon which is used generally as a vacuum grease.

The test pressure was raised in 34. 5-newton-per-square-centimeter (50-psia) increments up to an initial maximum pressure of 207 newtons per square centimeter (300 psi), which corresponds to the operating chamber pressure. A stabilizing period of about 1 minute was allowed between pressurizing steps. When the maximum pressure was reached, a short waiting period was maintained, and then the pressure was released. Following this test, a Kaiser effect check was made by repeating the pressurized monitoring. The Kaiser effect is the irreversible characteristic of acoustic emission resulting from an applied stress. If the effect is present, there is little or no acoustic emis-

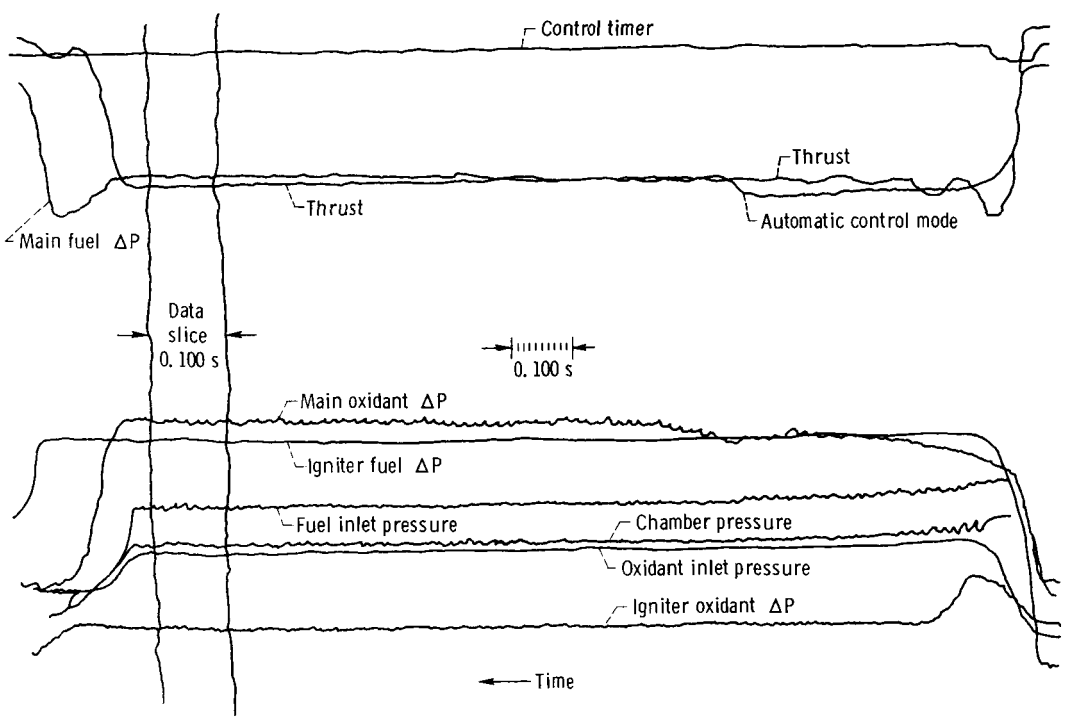

Figure 15. - Typical steady-state test trace (1. 5 s).

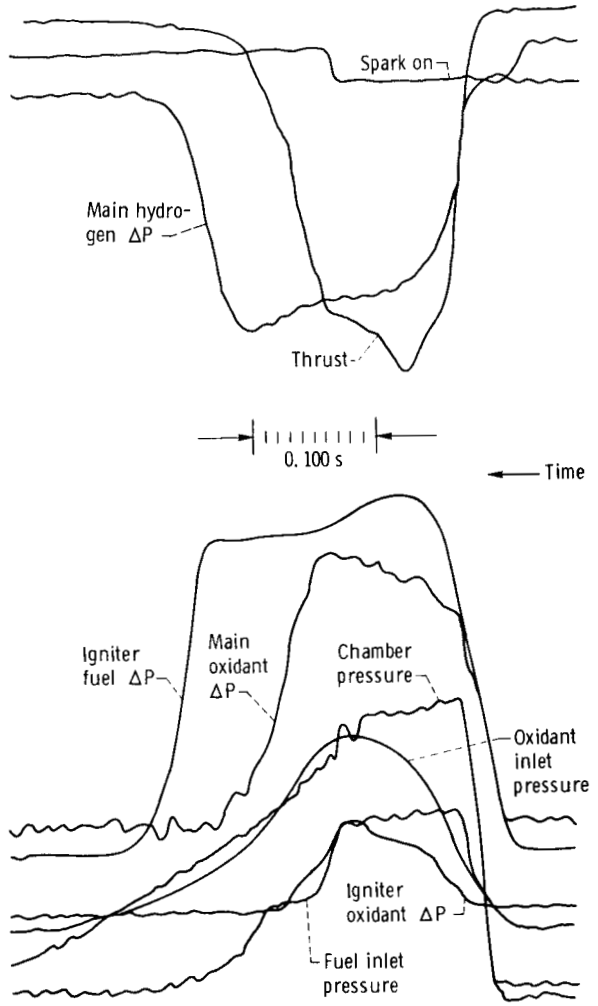

Figure 16. - Typical pulse-mode trace (17 540th pulse; duration, 0.100 s).

sion until previously applied stress levels are exceeded.

As the ACPS acquired pulses, the maximum acoustic emission test pressure was gradually increased until a pressure of 290 newtons per square centimeter (420 psi) was reached. This value was chosen to keep the test pressure slightly below 1.5 times the chamber pressure. This pressure was used during the remaining tests as the maximum and was never exceeded. Figure 17 is a typical trace obtained after 32 969 pulses showing the counts received from both the chamber and the manifold. In general, they were very low, which indicates essentially no significant acoustic emission activity. The zero emissions count during pressurization indicates the existence of the Kaiser effect.

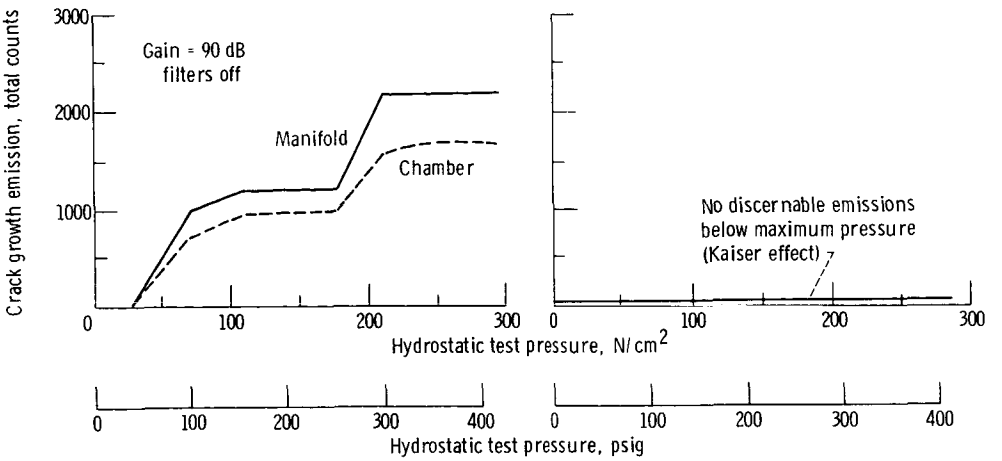

Figure 17. - Acoustic emission test of ACPS injector and chamber after 32 969 pulses.

RESULTS AND DISCUSSION

As previously mentioned, the primary objective of this program was to obtain data on the performance, thermal and hydraulic characteristics, pulse response, and cyclic life. Correlation and comparison of our data with the contractor's data were made, when applicable, and areas not thoroughly covered by the contracts program were evaluated, such as main propellant valves and valveless igniter thruster operation. Specifically, the Aerojet tested two ACPS engines and demonstrated a steady-state specific impulse of 4266 newton-seconds per kilogram (435 s) and a 3609-newton-second-per-kilogram (368 s) specific impulse at a 27.2 kilogram-second (60 lb-s) impulse bit as reported in reference 13. The Aerojet testing was terminated after an accumulation of 2513 seconds on one engine and 42 266 pulses on another.

Performance Characteristics

The performance model recommended by the JANNAF Performance Standardization Working Group (ref. 14) was used in this program to the extent that it was applicable to the film-cooled design tested. In the performance testing of the Lewis engine, attempts were made to verify Aerojet's results. Because the same method of measuring chamber pressure was used, this parameter was used as a quantitative check on performance and as a qualitative check on pulse repeatability. A comparison of the characteristic exhaust velocities was made. At the nominal mixture ratio of 4.0, a difference of 0.5 percent between the Aerojet data and the Lewis data was noted (fig. 8). Both sets of data exhibited the same negative slope with increasing mixture ratio.

In steady-state operation the characteristic exhaust velocity efficiency η_{C^*}, based on shifting equilibrium for ACPS S/N 003 was 93 percent (corrected for momentum loss and inlet temperatures) at a mixture ratio of 4.0. Standard deviation for the data is shown in figure 18. A list of the steady-state operating conditions and performance levels is shown in table IV. Note that η_{C^*} remains approximately constant throughout the pulse testing. In other words, no performance degradation was noticed for the ACPS thruster. These results were consistent with the ALRC tests (ref. 13).

TABLE IV. - PERFORMANCE LEVEL THROUGHOUT PROGRAM

316 Test	Chamber pressure		Mixture ratio O/F	Characteristic exhaust velocity, C*				Efficiency, η_{C^*}	Number of pulse counts
				Theoretical[b]		Experimental			
	N/cm^2	psia	(a)	m/s	ft/s	m/s	ft/s		
4	200	290	3.5	2492	8176	2366	7764	92.8	4
5	194	281	3.7	2484	8150	2293	7523	92.2	5
7	195	282	5.0	2395	7856	2222	7289	94.9	7
12	211	306	2.7	2480	8137	2466	8090	99.4	41
13	199	289	3.8	2475	8120	2212	7258	89.3	42
14	199	289	4.7	2430	7974	2246	7370	92.2	43
16	205	297	3.8	2485	8153	2290	7513	92.1	214
18	206	298	3.9	2478	8131	2293	7524	92.5	327
19	206	298	3.8	2485	8153	2295	7529	92.2	896
21	205	297	3.9	2484	8150	2290	7514	92.2	1 808
22	209	303	3.8	2489	8167	2305	7562	92.0	3 099
23	202	293	4.8	3420	7939	2199	7215	90.9	3 721
24	208	301	3.7	2497	8191	2373	7787	95.1	7 102
26	208	302	4.0	2481	8141	2312	7586	93.1	10 439
27	211	306	3.7	2495	8186	2387	7831	95.7	13 219
28	210	304	4.3	2455	8056	2319	7607	94.4	17 537
29	204	296	3.9	2479	8133	2278	7474	91.9	21 737
34	206	299	4.1	2469	8101	2276	7467	92.1	25 405
35	204	295	4.5	2446	8025	2241	7352	91.6	27 892
36	207	300	4.2	2464	8084	2313	7590	93.9	30 186
38	209	303	4.2	2464	8083	2329	7640	94.5	32 971
39	206	298	4.4	2447	8028	2254	7395	92.1	36 683
41	209	303	4.2	2462	8078	2329	7641	94.6	40 267
42	211	306	4.2	2466	8089	2373	7787	96.2	43 501
43	209	303	4.3	2455	8055	2310	7578	94.1	43 502
47	206	299	4.2	2464	8083	2292	7519	93.0	51 003
49	206	299	4.1	2472	8109	2293	7523	92.8	51 005

[a]Rounded-off parameters, C*theor. calculated directly from S. Gordon's (ref. 18).

[b]Shifting equilibrium.

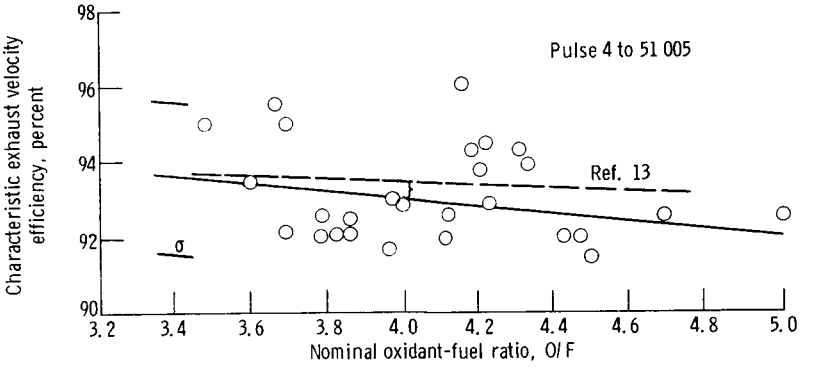

Figure 18. - ACPS performance (efficiency as function of mixture ratio.)

Thruster Life

Analytical predictions. - Aerojet (ref. 13) analytically predicted the critical fatigue stations in the ACPS injector and chamber components. The most critical location was predicted to be the coolant lip plane (station 4) of the thrust chamber. In this region a large thermal strain could be induced during the start transient by a high wall temperature on the gas side and a low wall temperature on the propellant side of the film cooling channels. This large ΔT is greatest on the initial pulse and diminishes with successive pulses, provided the chamber has insufficient time to cool down either naturally or by forced convection (H_2 lag at cutoff). By analytically forcing the thruster to cool down between pulses and analyzing this condition. Aerojet predicted a life of 50 000 deep thermal pulses at the coolant lip.

In support of this test program, further analytical life predictions were performed using the NASA Lewis Rocket Engine Thermal Strain Computer program (RETSCP; ref. 15). First, the rocket chamber throat station, which was a thin shell (0.018 in.) made of Haynes 188 and having the estimated thermal profile shown in figure 19 was analyzed. The analytical prediction for the number of cycles to failure at this station was determined to be 220 000 pulses at elevated temperatures (as shown in fig. 20), based on a predicted strain range of 0.236 percent.

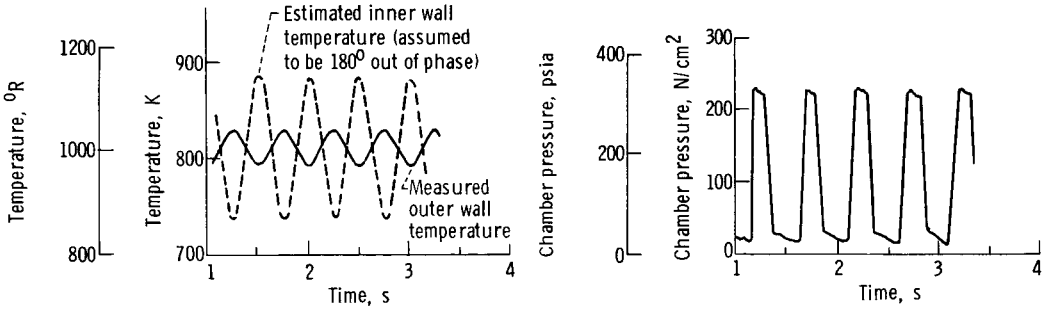

Figure 19. - ACPS thruster test conditions.

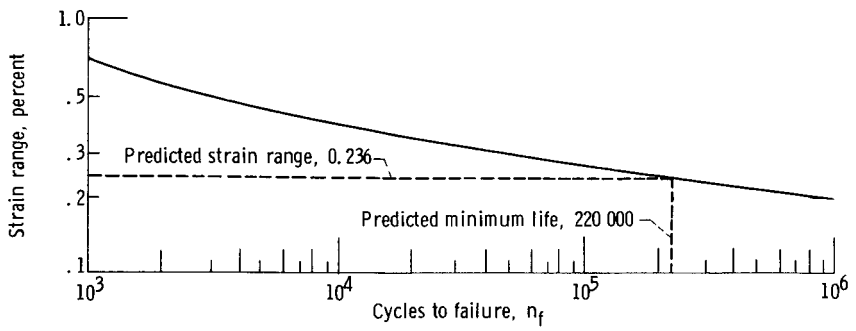

Figure 20. - Minimum fatigue life for Haynes 188 at elevated temperature.

The overall program was terminated before a similar analysis at the coolant lip station could be completed. Nevertheless, documentation of the model and sample cases (similar cross sections) for low-cycle thermal fatigue of rocket thrust chambers was completed under contract and is reported in reference 16.

Empirical determination. - To experimentally determine the thermal strains and corresponding thermal fatigue life, the thermal profile of the thruster was obtained

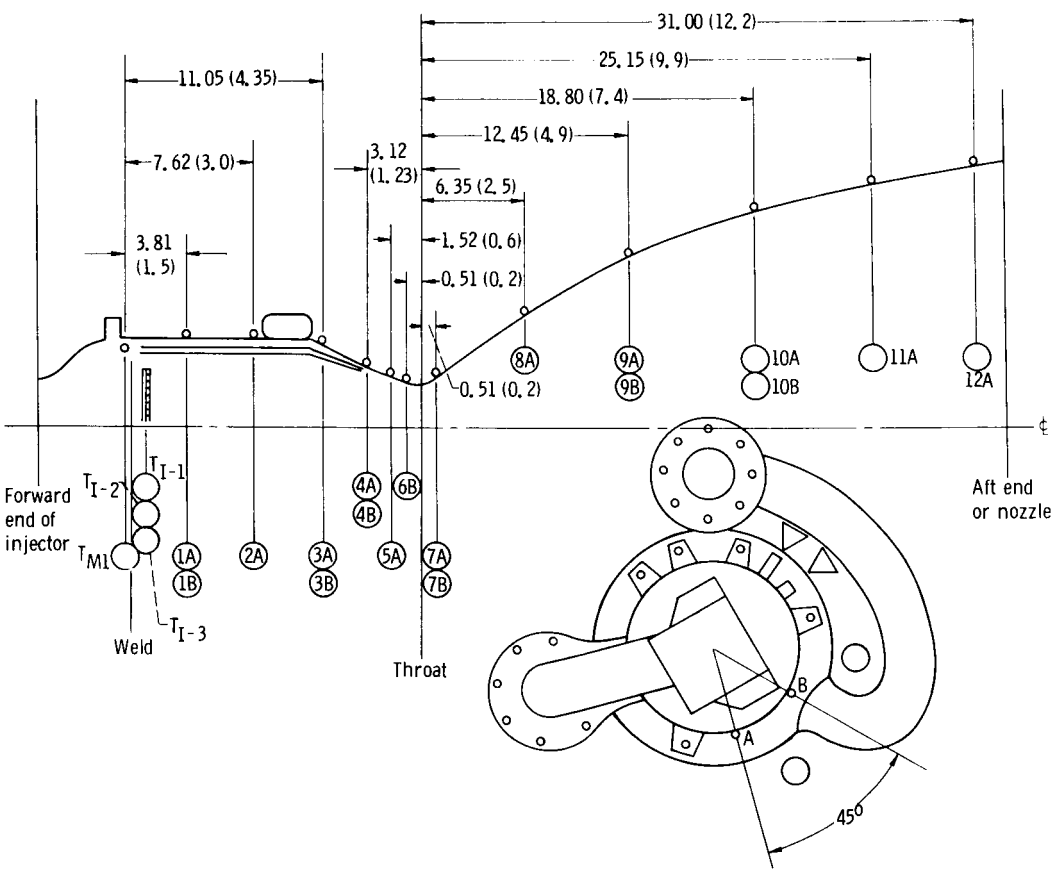

Figure 21. - ACPS thermocouple locations. (All dimensions are in cm (in.).)

with thermocouples (fig. 21). It was not possible to keep all of the thermocouples operative throughout the test series, but no test slot was initiated unless at least one thermocouple per axial station was operative. However, if that thermocouple failed during the test slot, the series was nevertheless completed. Table V shows the operating characteristics during the 660-second steady-state test.

As previously mentioned, Aerojet (ref. 13) analytically predicted a thermal fatigue cycle life of 50 000 deep thermal pulses, based on the large ΔT associated with startup. The test procedure for the NASA program was planned to simulate this deep thermal cycling as opposed to the duty cycle imposed on the Aerojet's ACPS thrusters. Consequently, a fuel lag of 0. 100 second following the 0. 100-second pulse was incorporated in the test procedure. The cooling of the thruster provided by this fuel lag plus the off-time of 0. 4 second between pulses produced the desired deep thermal cycling. In addition, long pulse-mode operation, usually greater than 25 to 50 pulses, increased the mean temperature of the various stations to the respective levels of a typical 1. 5-second steady-state test. This increase in wall temperature was also a severe condition to impose on the thruster as the physical and mechanical properties of the chamber materials decrease with increases in temperature. Hence, a corresponding decrease in cyclic life would be noted.

An important factor to be considered in testing of this nature was consistency of the pulses throughout the 51 000-pulse test series. As previously mentioned, the maximum chamber pressure for each pulse was recorded and served as the sampling point for a data slice. By noting this peak chamber pressure P_c value and by calculating a mean and standard deviation for each pulse series (lengths of 10 to 2000), an indication of the precision of the experiment was determined. Figure 22 indicates that throughout the test series, a mean P_c of 241 newtons per square centimeter (350 psia) and a σ standard deviation of 4. 14 newtons per square centimeters (±6 psia) occurred. It must be noted that the recorded P_c was actually the igniter oxidizer inlet pressure. With the igniter off, this was a true measure of main chamber pressure. However, because the igniter was firing throughout each pulse, the indicated pressure would be higher. The nominal value for P_c with the igniter firing was readily determined from the initial 1. 5-second test during each test slot.

As further evidence of pulse repeatability, the recorded traces for initial and final pulses of a typical 2000 pulse firing are shown in figure 23. These traces can be compared with traces of typical pulse firings at 900, 25 505, and 50 000 pulses shown in figure 24. Again, except for calibration changes and instrument response characteristics, the pulses were consistent.

TABLE V. - ATTITUDE CONTROL PROPULSION SYSTEM OPERATING CHARACTERISTICS FOR 660 SECOND TEST

Time	Chamber pressure		Mixture ratio, O/F	Characteristic exhaust velocity efficiency, η_{C^*}, percent	Propellant temperature				Thrust		Injector temperature								Chamber temperature											
					Oxygen		Hydrogen		N	lbf	Inlet, TMI		Face 1, TI-1		Face 2, TI-2		Face 3, TI-3		T_1		T_2		T_3		T_4		T_6		T_7	
	N/cm^2	psia			K	°R	K	°R			K	°R	K	°R	K	°R	K	°R	K	°R	K	°R	K	°R	K	°R	K	°R	K	°R
5	201	291	4.3	95.9	283	509	---	306	4933	1109	142	256	323	582	329	528	214	386	291	523	294	529	282	508	361	650	496	892	453	815
14	206	299	4.1	92.8	283	509	169	304	5031	1131	106	191	323	582	338	608	230	414	264	475	282	508	286	514	476	857	621	1135	668	1203
250	203	294	4.3	91.1	284	512	155	279	5026	1130	184	331	342	616	351	632	211	380	277	498	300	540	267	480	437	787	593	1067	723	1302
500	203	294	4.1	91.1	284	512	153	276	5022	1129	182	328	346	623	356	641	242	436	281	566	307	552	263	473	422	760	553	995	711	1279
1000	200	290	4.1	90.5	284	511	153	275	4978	1119	187	337	349	629	359	647	252	454	287	517	313	563	263	473	421	575	552	993	---	----
1500	206	298	3.9	93.4	283	510	151	272	4978	1119	168	302	352	634	364	655	326	587	288	519	319	574	259	467	426	767	567	1021	678	1221
2000	205	297	3.8	92.6	283	509	151	272	4995	1123	171	308	356	631	366	659	361	650	292	525	326	586	256	460	426	767	563	1014	690	1242
2500	201	292	3.9	89.9	282	507	152	274	4951	1113	199	359	354	638	367	661	387	697	245	531	323	581	252	453	426	767	538	968	693	1248
3000	206	298	3.7	93.2	↓	508	146	262	4942	1111	209	377	358	377	366	658	367	660	298	537	329	592	357	463	433	780	541	974	684	1230
3500	204	296	3.8	92.0		508	152	273	4960	1115	175	315	357	643	368	663	384	691	302	544	334	601	249	449	427	769	539	970	681	1225
4000	202	293	3.8	90.0		507	150	270	4953	1109	165	297	358	645	369	665	386	694	304	548	335	603	253	455	403	724	535	963	677	1218
4500	203	294	3.7	91.5		508	144	260	4938	1110	202	363	358	645	371	668	286	515	304	548	335	603	256	460	434	782	534	962	677	1219
5000	206	298	3.7	92.7		507	144	260	4915	1105	225	405	359	647	373	671	388	699	303	545	333	599	252	453	423	761	558	1004	686	1235
5500	203	294	3.7	91.2		507	143	258	4911	1104	182	327	360	648	371	668	397	714	182	539	329	592	257	462	430	774	543	977	669	1204
6000	201	291	3.8	90.5		508	151	271	2915	1105	194	350	359	646	372	670	359	646	296	532	325	585	254	457	418	753	543	977	678	1220
6500	206	299	3.7	93.5		508	146	262	4964	1116	129	233	361	650	372	670	392	705	294	529	317	571	261	470	424	763	534	962	663	1173
6600	204	296	3.7	92.2	↓	508	143	258	4933	1109	129	233	361	650	373	672	406	731	297	534	322	580	261	469	426	767	541	974	667	1200

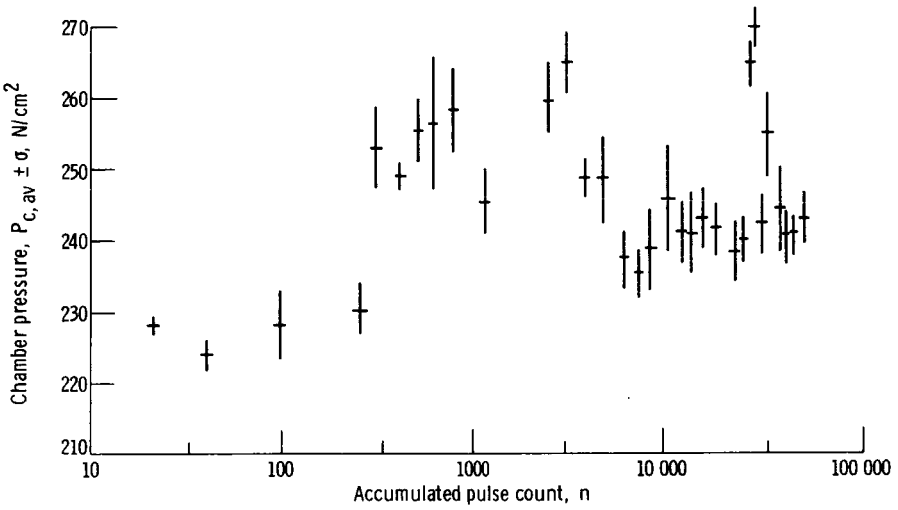

Figure 22. - Pulse deviations.

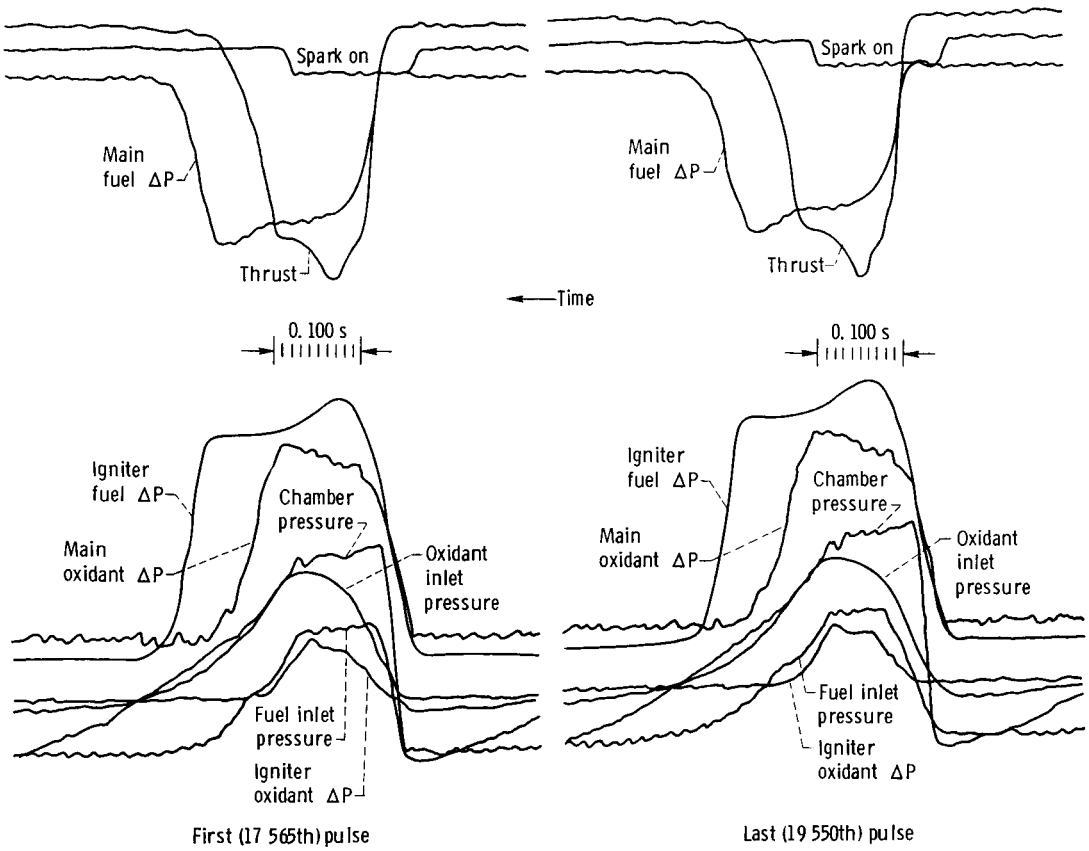

Figure 23. - Pulse repeatability (2000 pulse train).

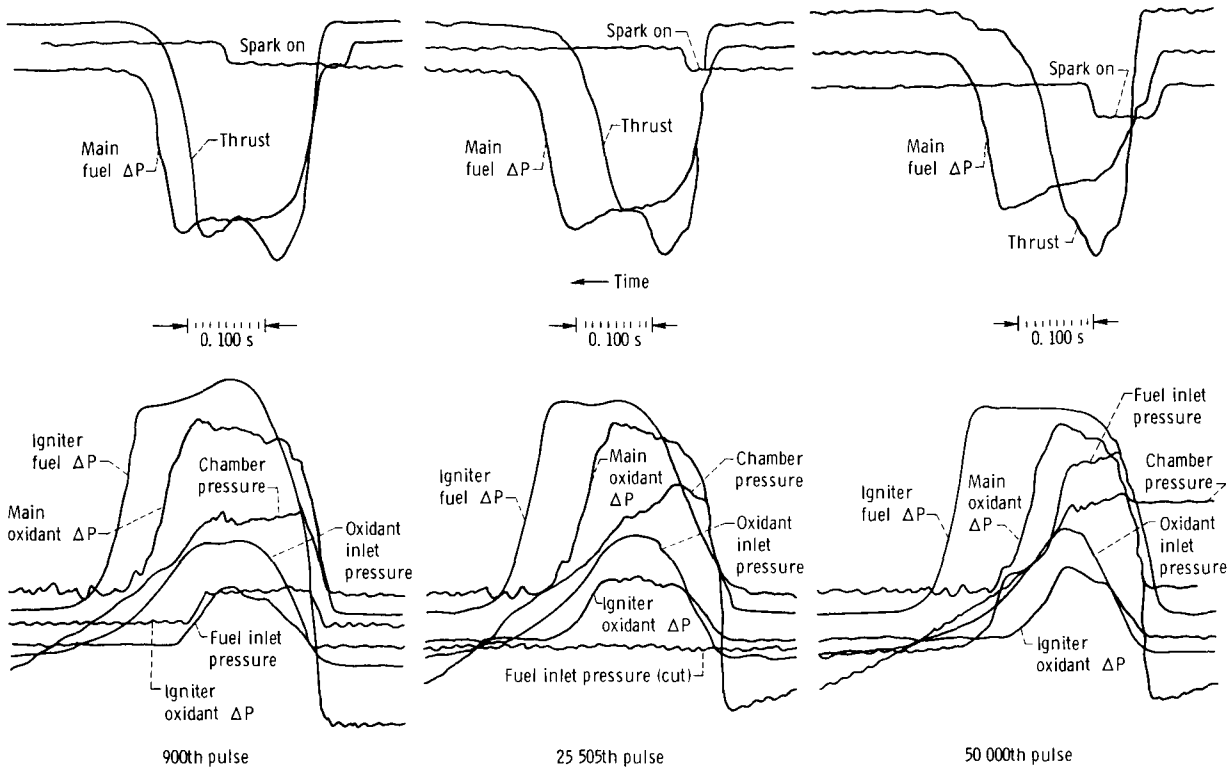

Figure 24. - Pulse degradation.

Specific Component History

The overall test history of the Lewis ACPS thruster is documented in tables VI and VII. Although each component will be discussed in detail a summary of some minor hardware or fabrication procedure modifications that should be incorporated to improve component life is presented here:

(1) Better inspection of main propellant valves to eliminate bellows weld cracks, thereby, eliminating valve leakage resulting from this type of failure.

(2) Igniter tip should be modified to incorporate alinement tabs.

(3) The ceramic on spark igniter package should be strengthened to eliminate cracking and, hence, potential plugging of igniter flow passages.

(4) Propellant routing should be modified to eliminate igniter oxidizer and fuel valves.

(5) Original thrust chamber design (ref. 13) and fabrication should be retained; thereby, insuring that chamber to throat section weld is located upstream of coolant lip axial station.

Igniter/exciter package. - During the test program, an internal short circuit occurred in the capacitance exciter package. This unit was returned to the vendor who determined the cause of failure to be a dielectric puncture of the insulation between the

TABLE VI. - TEST HISTORY

Pulses	Time, s	Chamber	Injector	Valves	Igniter	Exciter	Event	Probable cause	Solution
10	7.0	X					Nozzle skirt ripped off at end	Flow separation	Change to sea-level nozzle
41	12.5		X				Coolent passages on injector face beginning to show	----------	----------
		X					Retaining ring for fuel orifice broke loose	----------	----------
212	42.3			X			Fuel valve opening irregular	----------	----------
236	45.8			X			Fuel valve operating irregular	----------	Replaced pilot valve on main fuel valve
3 048	547.9				X		Burned tip on igniter tube	----------	Replaced tube S/N 004 with S/N 001
						X	Exciter unit not sparking	Internal short	Replaced unit S/N 002 with S/N 005
3 720	650.2			X			Fuel valve not closing	Bellows in valve leaking	Removed S/N 0014; installed S/N 001
						X	Ceramic cracked on exciter unit	----------	Replaced unit S/N 005 with S/N 004
4 567	778.6	X					Copper coolant ring tips turning rough	----------	----------
					X		Igniter oxygen line burned a hole	----------	Replaced with copper line
21 736	2771.0		X				Cracks on injector coolant passages around ignitor	----------	----------
					X		Cracks on igniter tube tip	----------	Replaced tube S/N 001 with S/N 004
25 402	3139.0					X	Ceramic cracked on exciter unit	----------	Replaced unit S/N 004 with S/N 008
26 578	3316.6				X		Igniter tube tip burned	----------	Replaced tube S/N 004 with S/N 002
30 185	3850.0				X		Igniter tube tip out of round and touching injector	----------	Straightened tube tip
30 688	3901.7	X					Cooling lip has two cracks on edge and 1 cm (1/8 in.) upstream	----------	----------
32 969	4129.84				X		Igniter tube scorched	----------	Replaced tube S/N 002 with repaired tube S/N 001 (centering pins)
36 682	4502.5	X					Crack at Haynes 188 to Armco weld upstream of throat; crack in Haynes 188 appearing inside chamber	High heat flux at weld	Rewelded
40 266	4860.9	X					Two cooling passages collapsing at cracks on lip	----------	----------
51 000	5944.8	X					Crack in Haynes 188 is more pronounced; not through the throat	----------	----------
		X					Three cooling passages collapsing at cracks on lip. Heating marks visible downstream of collapsed passages	----------	----------

power rectifier terminal and case ground. This mechanical failure was repaired by replacing the insulation sheet and adding a fiberglass barrier. This was the only failure noticed on any of the four exciters tested. Nevertheless, a failure of this type would not be tolerable in a real application. Exciter failures can be minimized by adequate quality control testing.

TABLE VII. - SUMMARY COMPONENT HISTORY

Component	Serial number	Total pulses	Total time, s
Injector/chamber	S/N 003	51 005/36 682	[a]6676
Main propellant valves:			
Hydrogen	S/N 0014	4 787	-----
Oxygen	S/N 0015	51 519	-----
Igniter tube	S/N 004	3 817	401
	S/N 001	19 417	5438
	S/N 004[b]	4 584	460
	S/N 002	6 727	672
	S/N 001[c]	17 042	1964
Spark exciter	S/N 002	3 765	582
	S/N 005	760	114
	S/N 004	21 718	2918
	S/N 008	25 353	2533

[a]Includes 660 s.

[b]Repaired; no centering pins added.

[c]Repaired; centering pin added.

A common failure with all of the igniter/exciter packages was the cracking of the thin ceramic insulator tip. Although this resulted in no apparent malfunctioning of the igniter, the insulator could break up into small pieces, lodge in the oxidizer orifices, and restrict the oxidizer flow. Based on these results, similar spark units for another test program were procurred with a redesigned (thicker) base and were successfully demonstrated (ref. 17).

Torch igniter. - The most frequently occurring problem with the torch igniter was cracking or scorching of the igniter tube tip (fig. 25). After replacement units were installed several times, a new feature, alinement tabs, was incorporated (fig. 26). These alinement tabs were machined 120^{o} apart and were sufficient to prevent radial movement of the tube due to temperature effects during testing. In addition, the concentricity of the igniter tube was now properly assured regardless of any possible assembly errors such as, nonuniform torquing.

The facility plumbing installation for the igniter coupled with the fast response igniter valves produced a hydraulic water hammer effect. This compression effect, during long pulse series, caused the stainless-steel tube to overheat and burn out. By installing a copper (water cooled) line, this potential facility failure was eliminated. In actual application, the igniter valves and the long feedline would be eliminated as discussed in the valveless igniter tests. Throughout the steady-state and pulse tests, none of the above ACPS igniter failures was of such magnitude as to abort a test series or result in any damage to any major ACPS thruster components.

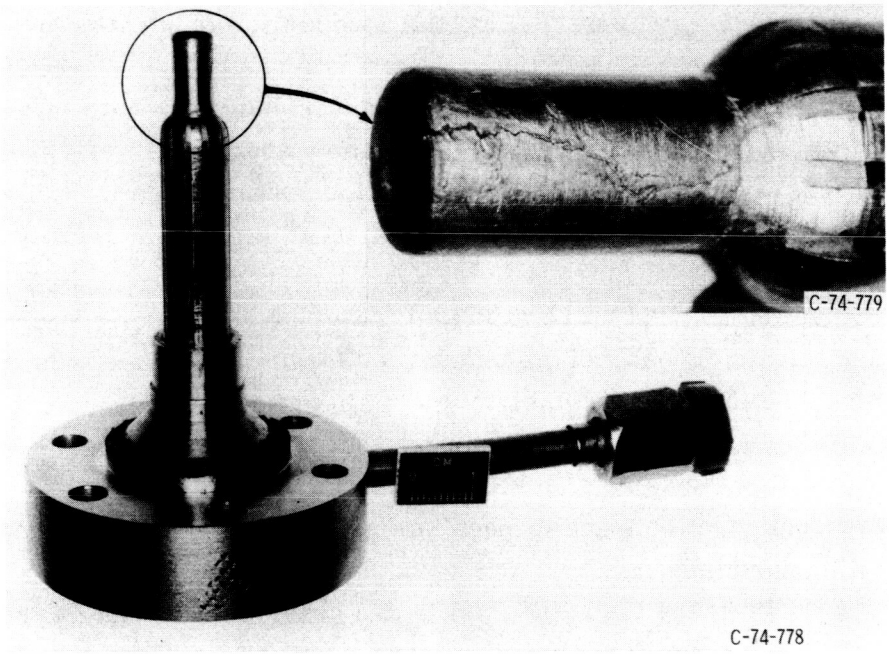

Figure 25. - Failed igniter tube tip after 19 415 pulses.

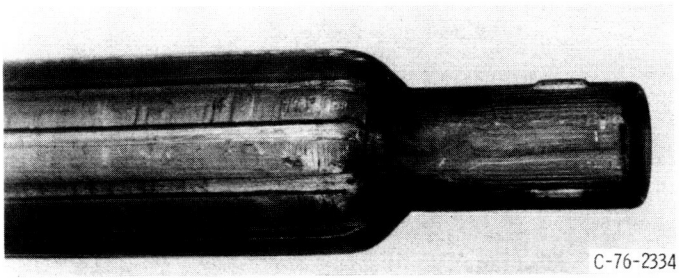

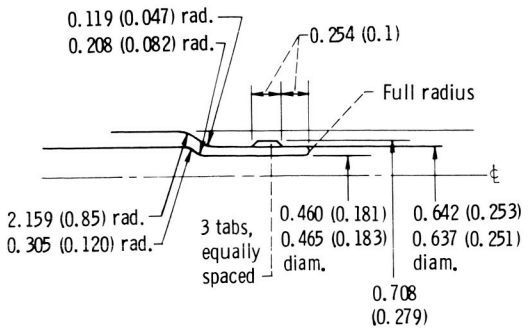

Figure 26. - Igniter tip modification. (Dimensions are in cm (in.).)

Main engine propellant valves. - A careful study of the fabrication of the valves revealed that no rigorous inspection of the bellows was made before assembly. Pinhole leaks, which were impossible to detect after valve assembly, grew to large detectable leaks after approximately 3700 actuations. Because these valves were pressure balanced, it was necessary to replace the fuel valve for continued testing. The replacement valve was a Flodyne ball valve that had been used in previous facility checkout tests.

The pilot valve for the fuel valve exhibited irregular response times, and disassembly revealed minute deposits of an unidentified foreign material. Cleaning eliminated the problem. Partial disassembly of the main propellant valve, which had accumulated over 51 000 actuations, indicated no degradation to the valve seat or poppet. The leakage rate was within the valve specifications. The difficulties experienced with the Marquardt valve configuration were inspection oriented and would be corrected for flight-weight, production hardware.

Chamber. - Preliminary tests and facility and chamber checkout, were made with a 40:1-area-ratio exhaust nozzle exhausting into a graphite-lined diffuser. During these tests with the facility hardware, it was difficult to maintain a sufficient chamber to diffuser seal and, hence, a sufficient back pressure for full flow of the nozzle. The diffuser-chamber seal was redesigned, and tests were begun on the 40:1 area ratio exhaust nozzle thruster under the condition that if the seal leaked appreciably, the thruster

C-73-4103

Figure 27. - Failed exhaust nozzle.

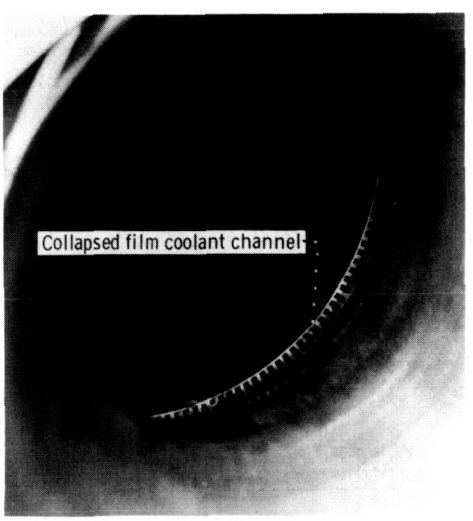

Figure 28. - Film coolant channel failures (32 969 pulses).

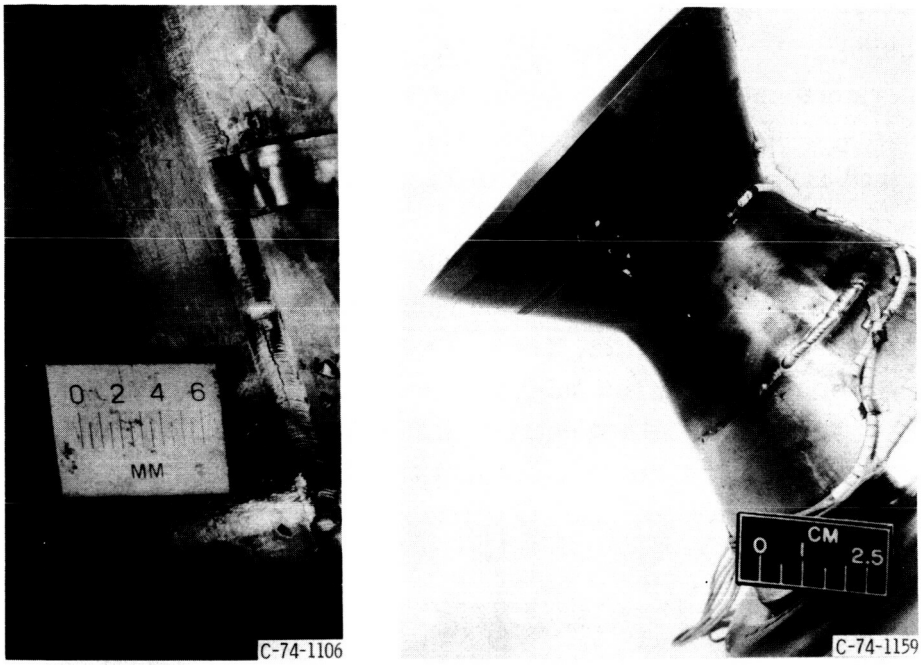

(a) Before 36 682 pulses. (b) Repair.

Figure 29. - Weld crack in convergent nozzle to throat section.

nozzle would be reconfigured to be fully expanded of sea-level conditions. Analysis of the axial thrust loads (ref. 14) indicated this change would not affect the results of the fatigue testing. After 4 steady-state tests and a 10 pulse series, the diffuser-chamber seal failed and the nozzle was damaged (fig. 27). The nozzle was then reconfigured to the appropriate sea-level area expansion ratio for the duration of the test program.

The internal copper combustion chamber exhibited cracks at the coolant lip as shown in figure 28. However, the cracks were not detrimental to the performance of the thruster. By the conclusion of the tests, three cracks had grown in size and permitted the channels collapse. Although chamber streaking was noted downstream of these channels, no change was noticed in performance nor was any chamber erosion noted.

At the end of the 15th test slot (36 682 pulses), the ACPS thruster was routinely removed for visual and acoustic emission inspection. Under hydrostatic loading of the chamber, acoustic emission monitoring indicated the existence of a crack somewhere on the thrust chamber. The test was stopped, and close visual inspection revealed a crack at the combustion chamber to throat section weldment (see fig. 29(a)).

During fabrication of the chamber, this welding was done after the zirconium-copper alloy liner was brazed to the steel shell. The weld location was made as far upstream of the throat as possible without jeopardizing the film cooling sleeve. This joint location was changed from the design location (upstream of the coolant lip) to eliminate

large ΔT's (strains) across the weld. However, this was a trade-off of ease of fabrication and temperature induced problems. Later versions of the ACPS thrust chamber will follow the original design. The weld crack (fig. 29) was repaired under "field" conditions. No degradation of the repair or local regions was noted during the remainder of the tests.

Injector. - One of the most important of all rocket-engine components is the injector because it must provide high combustion performance, uniform-combustion gas-temperature profiles, and long life. The ACPS injector successfully met all of these requirements. Slight cracking and bulging of the coolant passages on the injector face were evident but were definitely not detrimental to the performance and life of the ACPS thruster. Photographs of the injector face and chamber surfaces at various stages of the tests are shown in figure 30.

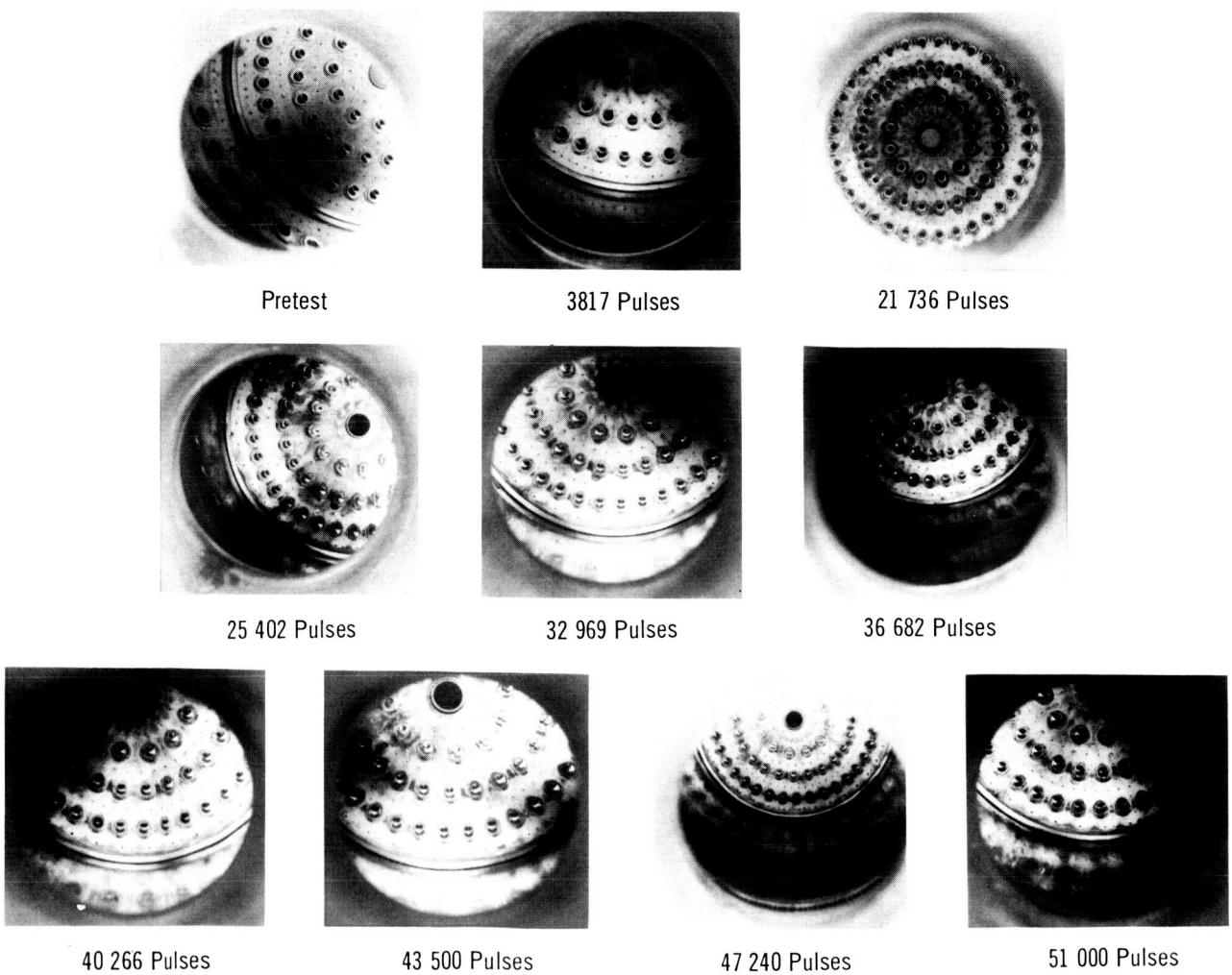

Figure 30. - Injector face after indicated number of pulses.

ACPS flight configuration (valveless igniter). - To reduce thruster weight and complexity, it was considered desirable to eliminate the igniter valves for a flight weight configuration. To verify that the thruster could be safely operated without igniter valves, a special test series was performed in which the igniter fuel and oxidizer valves were removed. The thruster was reconfigured by tapping off the igniter propellant supply immediately downstream of the main propellant valves. Flow control orifices, 0.243-centimeter (0.096 in.) in diameter and 0.226 centimeter (0.089 in.) in diameter, were installed in the respective igniter oxidizer and fuel lines. The timing change necessary to achieve a smooth ignition is shown in figure 14(c). The thruster response time (start signal to 90 percent thrust) was 38 milliseconds with a gradual ramping of chamber pressure. No tendency was noted toward hard starts or flow instabilities as a result of this modification.

Nondestructive Evaluation

Acoustic emission has been evaluated as a nondestructive method of detecting bond separations in rocket-engine thrust-chamber coolant passages. Reference 18 discusses the work with electroformed nickel to Nickel 200 bonds and also Inconel 600 to Nickel 200 brazed and diffusion bonded bonds. These results for acoustic emission were promising enough that this work was extended for copper to copper and copper to nickel bonds (see ref. 19).

This ACPS program used these results and attempted to extend the use of acoustic emission to detecting cracks in the cycled thrust chamber. Crack growth is depicted schematically in figure 31. As the crack propagates there is a moving series of zones; the process zone at the crack tip, the plastic zone surrounding the tip of the expanding crack, the elastic zone beyond this region, and the yielding zone, which is the transition between the plastic and elastic zones. The stress wave emanating from the expanding crack is detected by the acoustic emission equipment.

For the thrust chamber an attempt was made to develop a plot of acoustic emission counts as a function of operational cycles. Figure 32 is a curve representing the ideal situation where imminent failure could be detected by the rapid rise in counts or count rate. The acoustic emission literature available (such as ref. 20) discusses related successful results for pressure vessel testing.

Figure 17 was a typical acoustic emission trace of the ACPS thrust chamber showing low activity, which indicates that no cracks were developing. Figure 33(a) is a trace from a test in which a crack in the weld was detected. At 27.6 newtons per square

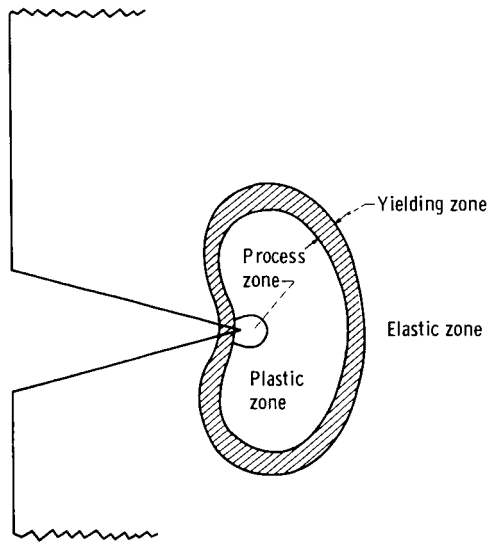

Figure 31. - Zone producing acoustic emission near crack tip.

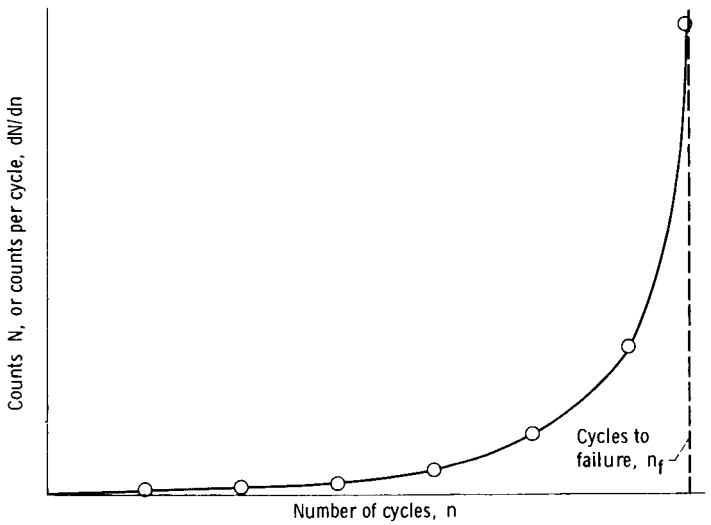

Figure 32. - Ideal acoustic emission failure prediction.

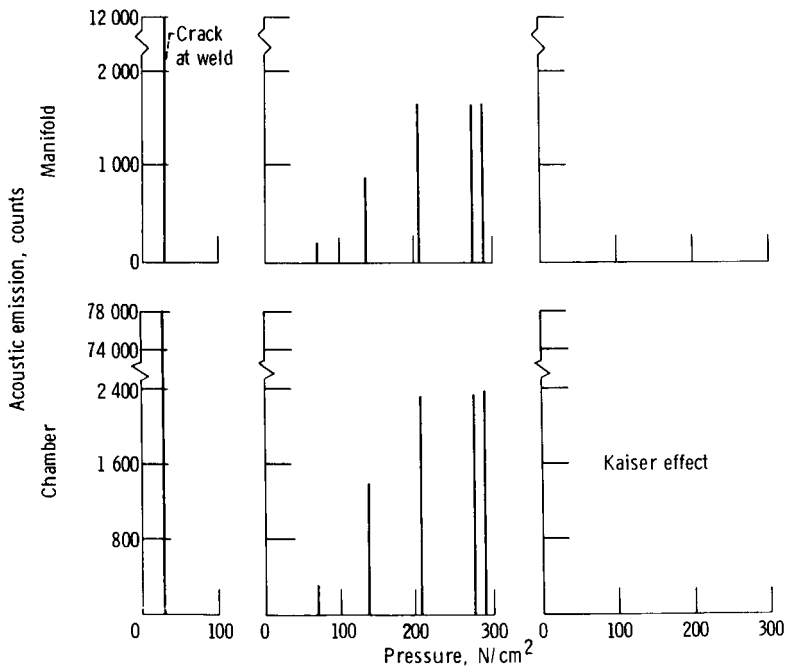

(a) After 36 692 pulses.

(b) After repair.

Figure 33. - Acoustic emission monitoring (chamber failure).

centimeter (40 psig) 78 000 counts were recorded from the transducer mounted on the chamber. For the manifold transducer only 13 000 counts were recorded, which indicates the attentuation of the signal by the various manifold welds. These high levels of counts greatly exceeded the usual 1000 to 200 counts, indicating a potential defect. The counters were reset, and the chamber was pressurized to 69 newtons per square centimeter (100 psig). At this point, more acoustic emission activity was detected and the test was stopped.

Although qualitative in nature, the results of the acoustic emission monitoring definitely indicated the existence of a defect after the 36 682 pulses. Close inspection by dye penetration located the weld crack discussed previously. After repairs of the weld, the chamber was again checked; the results are shown in figure 33(b). The low counts were similar to those from the chamber before the weld crack and indicate a structurally sound chamber.

Figure 34 shows the attempt to construct a curve similar to that of figure 32. Total accumulated counts are plotted as a function of accumulated engine pulses. The solid bars indicate the counts recorded during the acoustic emission test, and the curve represents total accumulated counts. The high-count bars before 10 000 pulses were reached were produced extraneously. Metal foil shields were tack welded onto the outside of the chamber to protect the thermocouples from heat during testing. During the acoustic emission tests, the pressurizing of the chamber was causing movement of the foils resulting in the extraneous counts. When the foils were removed, the extraneous counts ceased as shown in figure 34. Examination of figure 34 shows a slight tendency towards a rise in total accumulated counts before the weld crack discovery. In general,

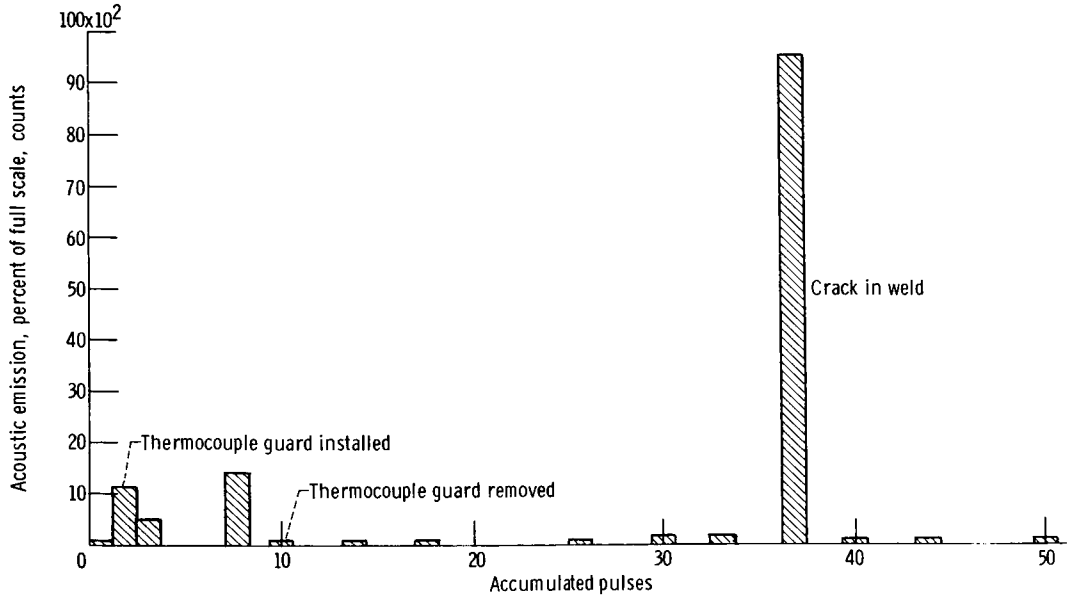

Figure 34. - Acoustic emission summary.

this curve did not result in the ideal type of curve like that of figure 32. However, it should be noted that this was the first attempt to use acoustic emission as an NDE technique for highly cycled thrust chambers. It was successfully used in a qualitative manner. If fully developed in a manner similar to acoustic emission for pressure vessel monitoring, this technique could be used for quick onboard or postflight monitoring of thrusters of this type. Crack growth, if occurring, could be detected and, if necessary, the chamber removed for repair or replacement.

CONCLUSIONS

These experimental test results, combined with those obtained under contract, have provided a base for the development of reliable, reusable attitude-control thrusters for the proposed all-cryogenic space-transportation vehicles. Specific conclusions were as follows:

1. Main propellant valves should be closely inspected to eliminate bellows weld cracks.

2. The igniter tip should be modified to incorporate alinement tabs.

3. The ceramic on the spark-igniter package should be strengthened to eliminate cracking and, hence, potential plugging of igniter flow passages.

4. Propellant routing should be modified to eliminate igniter oxidizer and fuel valves.

5. The original thrust chamber design and fabrication should be retained, thereby insuring that chamber to throat section weld is located upstream of coolant lip sectional plane.

6. The nondestructive examination technique, acoustic emission, should be considered as a good, qualitative, diagnostic tool for the ACPS thrusters. The concept would be excellent for quick postflight inspection of individual thrusters without removing the part from the flight vehicle.

Lewis Research Center,
National Aeronautics and Space Administration,
Cleveland, Ohio, January 4, 1977,
506-21.

REFERENCES

1. Senneff, J. M.: High Pressure Reverse Flow APS Engine. (BELL-8636-950004, Bell Aerospace Co.; NAS3-14353), NASA CR-120881, 1972.

2. Paster, R. D.: Hydrogen-Oxygen APS Engines. Vol. 1: High Pressure Thruster. (R-8837-1-Vol-1, Rocketdyne; NAS3-14352) NASA CR-120805, 1973.

3. Lauffer, J. R.: Space Shuttle Auxiliary Propulsion (APS) Ignition System. (R-8724, Rocketdyne; NAS3-14351) NASA CR-72972, 1971.

4. Smith, G. M.: High-Performance Space Shuttle Auxiliary Propellant Valves. (R-9078, Rocketdyne; NAS3-14350) NASA CR-120976, 1973.

5. Johnson, R. J.: Investigation of Thrusters for Cryogenic Reaction Control Systems. Vol. 1. (TRW-09849-6001-R0-00 - Vol. 1, TRW Systems Group; NAS3-11227) NASA CR-72784, 1970.

6. Johnson, R. J.: Investigation of Thrusters for Cryogenic Reaction Control Systems. Vol. 2: Appendices. (TRW-09849-8002-R0-00-Vol. 2, TRW Systems Group; NAS3-11227) NASA CR-72785, 1970.

7. Johnson, R. J.: Hydrogen-Oxygen Catalytic Ignition and Thruster Investigation. Vol. 1: Catalytic Ignition and Low Pressure Thruster Evaluations. (TRW-14549-6001-R0-00-Vol.-2; TRW Systems Group; NAS3-14347) NASA CR-120870, 1972.

8. Johnson, R. J.; Heckert, B.; and Burge, H. L.: Hydrogen-Oxygen Catalytic Ignition and Thruster Investigation. Vol. 2: High Pressure Thruster Evaluations. (TRW-14549-6001-R0-00-Vol.-2; TRW Systems Group; NAS3-14347) NASA CR-120870, 1972.

9. Wichmann, H.: Advance Technology for Space Shuttle Auxiliary Propellant Valves. (S-1261, Marquardt Corp.; NAS3-14349) NASA CR-120975, 1973.

10. Hydrogen-Oxygen Auxiliary Propulsion for the Space Shuttle. Vol. 1: High Pressure Thrusters. (Aerojet Liquid Rocket Co.; NAS3-14354) NASA CR-120895, 1973.

11. Rosenberg, S. D.; et al.: Ignition Systems for Space Shuttle Auxiliary Propulsion System. (ALRC-1678-26-F, Aerojet Liquid Rocket Co.; NAS3-14348) NASA CR-72890, 1972.

12. Gregory, J. W.; and Herr, P. N.: Hydrogen-Oxygen Space Shuttle ACPS Thruster Technology Review. AIAA Paper 72-1158, Dec. 1972.

13. Integrated Thruster Assembly Program. (Aerojet Liquid Rocket Co.; NAS3-15850) NASA CR-134509, 1973.

14. JANNAF Rocket Engine Performance Prediction and Evaluation Manual. CPIA-Publ-246, Chemical Propulsion Information Agency, 1975.

15. Miller, Roy W.: RETSCP: A Computer Program for Analysis of Rocket Engines Thermal Strains with Cyclic Plasticity. (Atkins and Merrill, Inc.; NAS3-17807) NASA CR-134640, 1974.

16. Miller, Roy W.: Cyclic Fatigue Analysis of Rocket Thrust Chambers. Vol. 2: Attitude Control Thruster High Cycle Fatigue. (Atkins and Merrill, Inc.; NAS3-17807) NASA CR-134641-Vol. -2, 1974.

17. Hannum, N. P.; Kasper, H. J.; and Pavli, A. J.: Experimental and Theoretical Investigation of Fatigue Life in Reusable Rocket Thrust Chambers. AIAA Paper 76-685, July 1976.

18. Malone, G. A.; Stauffis, R.; and Wood, R.: Nondestructive Tests of Regenerative Chambers. (BAC-8654-953003, Bell Aerospace Co.; NAS3-14376) NASA CR-120980, 1972.

19. Malone, G. A.; Vecchies, L.; and Wood, R.: Nondestructive Tests of Regenerative Chambers. (BAC-8654-953005, Bell Aerospace Co.; NAS3-16800) NASA CR-134656, 1974.

20. Spanner, J. C.; and McElroy, J. W., eds.: Symposium on Monitoring Structural Integrity by Acoustic Emissions. ASTM STP 571, Am. Soc. Test. Mater., 1975.

NASA-Langley, 1977 E-8981